Received: 16 April 2020 | Revised: 21 August 2020 | Accepted: 31 August 2020

DOI: 10.1002/ar.24545

ARTICLE

The Anatomical Record | WILEY

# Appendicular skeletal morphology of North American *Martes* reflect independent modes of evolution in conjunction with Pleistocene glacial cycles

**Leigha M. Lynch**[1,2] | **Ryan Felice**[3] | **Haley D. O'Brien**[1]

[1]Anatomy and Cell Biology, Oklahoma State University Center for Health Sciences, Tulsa, Oklahoma

[2]Neuroscience, Washington University in St. Louis School of Medicine, St. Louis, Missouri

[3]Cell and Developmental Biology, University College London, London, United Kingdom

**Correspondence**
Leigha M. Lynch, Oklahoma State University Center for Health Sciences, 1111 W. 17th St., Tulsa, OK, 74107.
Email: lynch.leigha.m@wustl.edu

**Funding information**
Oklahoma State University Robberson Summer Graduate Research Fellowship; Oklahoma State University Women's Faculty Council Research Award; Sigma Xi Grants in Aid of Research

## Abstract

Pleistocene glacial cycles are thought to have driven ecological niche shifts, including novel niche formation. North American pine martens, *Martes americana* and *M. caurina*, are exemplar taxa thought to have diverged molecularly and morphologically during Pleistocene glaciation. Previous research found correlations between *Martes* limb morphology with biome and climate, suggesting that appendicular evolution may have occurred via adaptation to selective pressures imposed by novel and shifting habitats. Such variation can also be achieved through non-adaptive means such as genetic drift. Here, we evaluate whether regional genetic differences reflect limb morphology differences among populations of *M. americana* and *M. caurina* by analyzing evolutionary tempo and mode of six limb elements. Our comparative phylogenetic models indicate that genetic structure predicts limb shape better than size. Marten limb size has low phylogenetic signal, and the best supported model of evolution is punctuational (kappa), with morphological and genetic divergence occurring simultaneously. Disparity through time analysis suggests that the tempo of limb evolution in *Martes* tracks Pleistocene glacial cycles, such that limb size may be responding to shifting climates rather than population genetic structure. Contrarily, we find that limb shape is strongly tied to genetic relationships, with high phylogenetic signal and a lambda mode of evolution. Overall, this pattern of limb size and shape variation may be the result of geographic isolation during Pleistocene glacial advance, while declines in disparity suggest hybridization during interglacial periods. Future inclusion of extinct populations of *Martes*, which were more morphologically and ecologically diverse, may further clarify *Martes* phenotypic evolution.

**KEYWORDS**

limb shape, limb size, mustelid, phylogenetic comparative methods

## 1 | INTRODUCTION

Climate is one of the most prominent extrinsic selective pressures influencing phenotypic evolution, as it often leads to shifts in environment that require adaptation or

Evolution of *Martes* limb shape and size.

  

migration in order for populations to persist (Andrews, 2010; Reznick & Travis, 2001). Glacial cycles during the Pleistocene epoch (2,580,000 to 11,700 years ago) provide a unique opportunity to study the phenotypic outcomes of organism-environment interactions across time scales encompassing more contemporary adaptive divergence (Hairston, Ellner, Geber, Yoshida, & Fox, 2005; Hendry, Farrugia, & Kinnison, 2008; Kinnison & Hairston, 2007; Kinnison & Hendry, 2001) and deeper-time ecological speciation (Funk, Nosil, & Etges, 2006; Rundle & Nosil, 2005; Schluter, 2000). These massive shifts in climate and available geographic area resulted in frequent reorganization of plant communities and the pursuant development of novel biomes throughout the Pleistocene (Jackson et al., 2000; Jackson & Overpeck, 2000; Shafer, Cullingham, CÔTÉ, & Coltman, 2010; Williams & Jackson, 2007). This series of primary and secondary succession events, in turn, resulted in the opening of niche space and the shifting of existing niches. Repeated ecological shifts broadly influence Pleistocene populations, as fluctuation in climate led to cycles of ice sheet expansion and contraction. Researchers have shown that in North America, some species of rodents, ungulates, and carnivorans tracked these shifting habitats and underwent phenotypic adaptation to these newly forming environments (e.g., *Tamiasciurus* (Arbogast, Browne, & Weigl, 2001), *Clethrionomys gapperi* (Runck & Cook, 2005), *Ovis dalli*, and *O. canadensis* (Loehr et al., 2006), *Canis lupus* (Muñoz-Fuentes, Darimont, Wayne, Paquet, & Leonard, 2009), *Oreamnos americanus* (Shafer, Côté, & Coltman, 2011)). North American pine martens, *Martes americana* and *M. caurina*, currently share the same biomes and geographic distribution of many of these aforementioned species (Nowak, 1999), suggesting that they may have experienced similar selective pressures and modes of evolution.

Indeed, genetic and fossil evidence supports the divergence and diversification of *M. americana* and *M. caurina* during Pleistocene glaciation (540 kya) (Figure 1, Lynch, 2019a), with *M. caurina* becoming established in coniferous forests of the Western coast of North America, and *M. americana* tracking northward into broadleaf and boreal forest (Figure 2). Therefore,

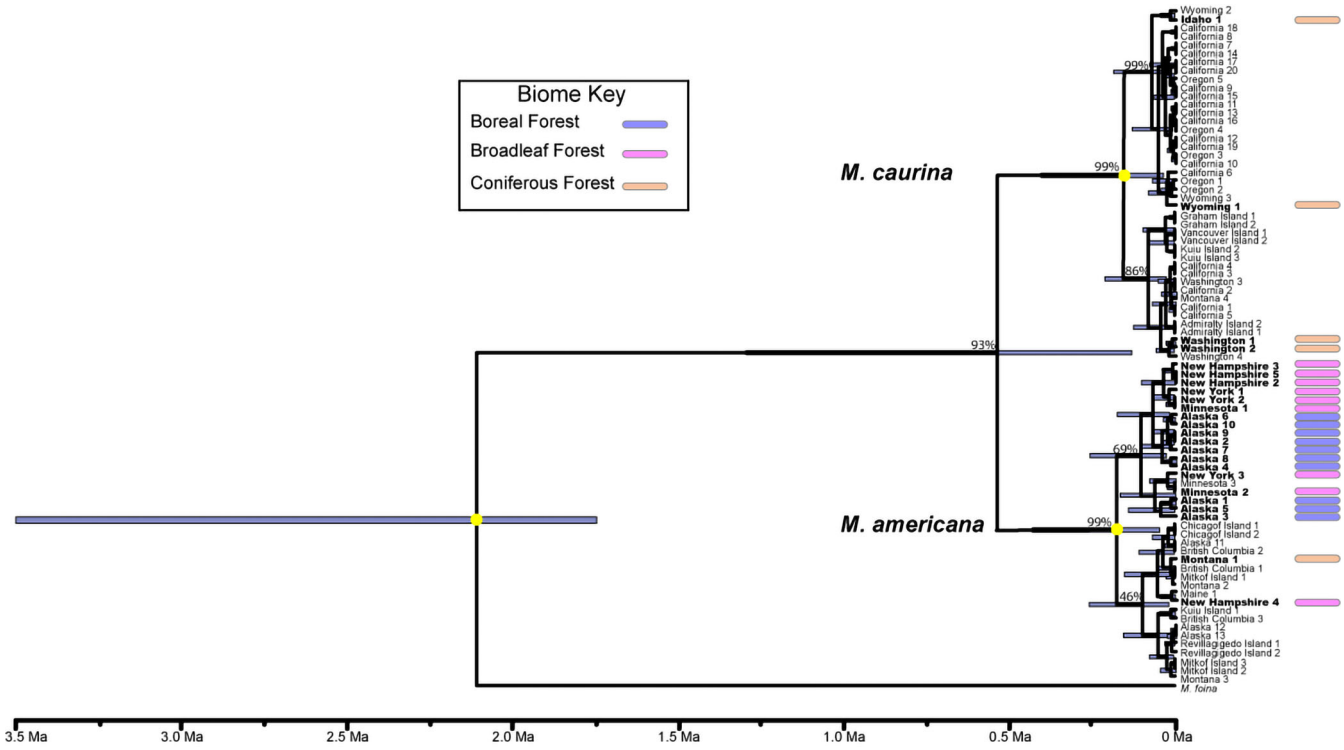


**FIGURE 1** Bayesian phylogeny of *Martes americana* and *M. caurina* specimens constructed from cytochrome b modified from Lynch (2019a). Branch lengths represent time and node values indicate posterior probability support. For full nodal support values see Supplemental S1 (Section C, Figure S1). Yellow circles denote nodes that were fossil calibrated (Lynch, 2019a). Purple bars on nodes represent the 95% confidence interval on node ages. The limb morphology was measured in each of the specimens whose names appear in bold. Purple, orange, and pink bars at the tree tips represent the biome from which specimens were collected, as indicated by the key to the left. Tip labels indicate the state from which specimens were collected followed by an individual specimen number. See Supplemental S1 (Section D, Table S1) for the collection number associated with each tip label

biogeography of North American martens is generally divisible by both species and habitat (although there are zone of hybridization [Stone, Flynn, & Cook, 2002; Dawson et al., 2017; Colella, Johnson, & Cook, 2018; Colella, Wilson, Talbot, & Cook, 2018]) in a pattern congruent with the last glacial retreat. Although they were once considered the same species (Clark, Anderson, Douglas, & Strickland, 1987), recent work has identified significant genotypic and phenotypic differences between *M. caurina* and *M. americana*. Limb skeletal morphology of these species has been found to significantly differ between not only species, but also among individuals inhabiting disparate biomes (Lynch, 2019b). When these observations are combined with marten biogeographic distributions (Figure 2), several patterns emerge for consideration. First, limb skeletal morphology varies by habitat: heterospecifically between *M. caurina* (endemic to coniferous forests) and *M. americana*, as well as conspefically within *M. americana* (between broadleaf and boreal forest populations). Second, the distribution of each species range, and metapopulations therein, follows glacial recession (Figure 2). Therefore, it is currently unclear if the differences in limb morphology reflect local adaptation to their unique habitats (selection) or stochastic changes that accompany the temporally-dependent accumulation of genetic variation (drift). Using a gene tree sourced from individuals belonging to non-hybridizing metapopulations (Lynch, 2019a) and phylogeny-based evolutionary modeling methods, we seek to determine whether these biome-linked differences in North American *Martes* limb skeletal morphology evolved via glacial-cycle-linked adaptive processes or whether limb evolution in this genus reflects an accumulative, stochastic process that may be the result of isolation and genetic drift.

Throughout the Pleistocene, climate underwent several temperature oscillations (Bond cycles) that greatly influenced the distribution of flora and fauna (Bond et al., 1993; Shafer et al., 2010). These fluctuations were marked by warm periods, called Dansgaard-Oeschger events, in which temperatures increased up to 16°C in just a decade (Lang, Leuenberger, Schwander, & Johnsen, 1999; Rahmstorf, 2002; Seierstad et al., 2014; Wolff, Chappellaz, Blunier, Rasmussen, & Svensson, 2010). During Dansgaard-Oeschger events, ice sheets retreated, allowing for geographic range expansion, effectively increasing and/or creating niche space (Dynesius & Jansson, 2000; Hewitt, 1996; Hewitt, 2004; Koch, Diffenbaugh, & Hoppe, 2004). These were then followed by Heinrich events during which climate cooled and ice sheets expanded across the Northern

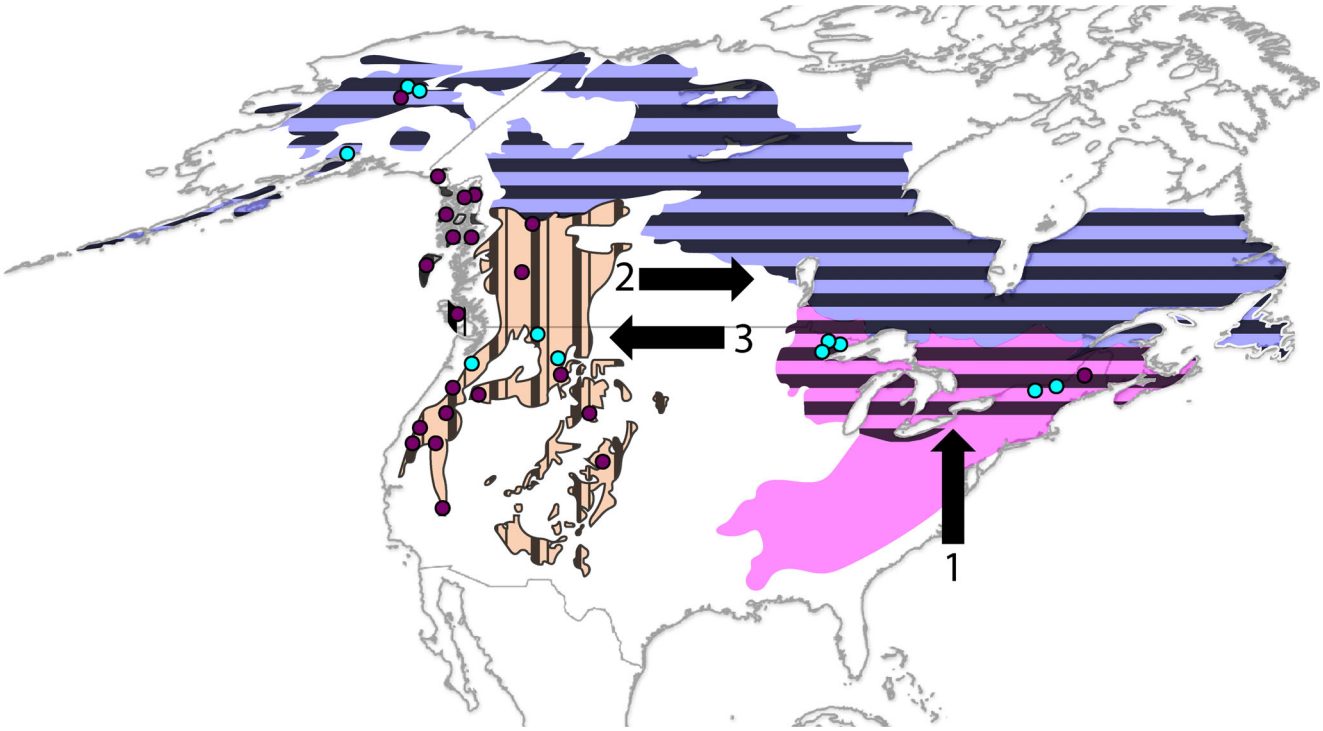


**FIGURE 2** Geographic distribution of *Martes americana* (horizontal lines) and *M. caurina* (vertical lines). Colors indicate the modern biome distributions. Purple are boreal forests; orange are coniferous forests; and pink are broadleaf forests. Points on the map indicate the geographic location from which specimens were collected. Teal points represent specimens that were both sequenced and whose morphology was measured. Burgundy points represent specimens whose sequences were collected from GenBank (NCBI) and used to construct the Bayesian phylogeny (Figure 1). Arrows and their associated numbers indicate the direction and order of glacial retreat at the end of the Pleistocene based on Dyke (2004)

hemisphere (Rahmstorf, 2002; Seierstad et al., 2014; Wolff et al., 2010). The proliferation of ice sheets then reduced the geographic area available to ecological communities, contracting niche space. The most recent of the North American Heinrich events were the Illinoian glaciation (191–130 kya) and the Wisconsin glaciation (80–11 kya) (Clark et al., 2009; Dyke, 2004; Edwards, Cheng, Murrell, & Goldstein, 1997; Rovey & Balco, 2011; Shackleton, Sánchez-Goñi, Pailler, & Lancelot, 2003; Stirling, Esat, Lambeck, & McCulloch, 1998). During these glacial periods, the expansion of ice sheets caused changes in local temperatures and precipitation that increased C4 plant abundance (Koch et al., 2004) and resulted in non-analog plant communities across the United States and Mexico (Gill, Williams, Jackson, Lininger, & Robinson, 2009; Williams & Jackson, 2007; Williams, Shuman, & Webb, 2001). The expansion of ice sheets also separated many populations of animals into isolated regions in the eastern and western United States, where they encountered novel forest and taiga habitats in both regions, and novel prey and predators (Jackson et al., 2000; Jackson & Overpeck, 2000; Williams & Jackson, 2007). Geographic isolation and behavioral modification in response to shifting selective pressures precipitated allopatric speciation of many animals, often resulting in a concurrent divergence of morphologies (see review in Shafer et al., 2010). After the last glacial maximum (LGM, 19 kya) (Clark et al., 2009), plant communities underwent a final reorganization that formed the modern biomes we see today (Williams & Jackson, 2007). Many species that were previously isolated in the eastern United States dispersed into these newly formed biomes, where many underwent phenotypic evolution (Lister, 2004; Milá, Smith, & Wayne, 2007; Zink & Dittmann, 1993).

North American pine martens, *M. americana* and *M. caurina*, are two candidate species with shifts in genetic diversity and morphological disparity that may be attributable to changes in climate and habitat during the Pleistocene. Based on mitochondrial DNA, researchers have proposed that these species underwent allopatric speciation coincident with Pleistocene glaciation (Colella, Wilson, et al., 2018; Dawson et al., 2017; Lynch, 2019a; Stone et al., 2002; Stone & Cook, 2002). Although the precise dates of their divergence and diversification are debated, fossil-calibrated gene-based phylogenies suggest that these species diverged during the Pre-Illinoian glacial episode and underwent diversification during the Wisconsin glaciation (Lynch, 2019a). Today, these species are found in three distinct biomes: (a) temperate broadleaf and mixed forest in the north-eastern United States and south-eastern Canada (*M. americana*); (b) temperate coniferous forest in the central and northern Pacific United States and Canada (*M. caurina*); and (c) boreal forest in central Alaska and northern Canada (*M. americana*) (Banfield, 1974; Clark et al., 1987; Nowak, 1999). The limb skeletal morphology of these species differs significantly between biomes and in correlation with climatic variables such as annual temperature and snowfall (Lynch, 2019b). This suggests that marten limbs may be adaptively plastic to extrinsic selective pressures that result from significant differences in habitat, such as vegetational substrate (e.g., deciduous broadleaf trees versus conifers) and the locomotory demands of snow absence, presence, and depth. It is also possible, however, that changes in postcranial phenotype reflect a stochastic accumulation of variance, as *M. americana* and *M. caurina* evolved in isolated habitats in the eastern and western United States during the Pre-Illinoian Pleistocene glaciation.

This study focuses on the evolution of appendicular skeletal morphology in North American *Martes* to determine whether limb shape and size evolved via adaptive mechanisms to biome, or due to stochastic mechanisms such as drift. We use limb shape and size as our evolutionary morphological model because it reflects locomotor mode, habitat, and substrate (Fabre et al., 2013; Fabre, Cornette, Goswami, & Peigné, 2015; Panciroli, Janis, Stockdale, & Martín-Serra, 2017; Polly, 2010; Samuels, Meachen, & Sakai, 2013). While the macroevolution of mustelid morphology has been studied using phylogenetic comparative methods (e.g., Law, 2019; Law, Slater, & Mehta, 2018a, 2018b), fewer studies have examined patterns of evolution at metapopulation, intra-specific, and/or temporally intermediate evolutionary levels (i.e., spanning micro-to-macro evolutionary scales). Using a phylogeny constructed from cytochrome b sequences collected from multiple specimens of *M. americana* and *M. caurina* from across their geographic ranges as a comparative framework (Lynch, 2019a), we tested two hypotheses: ($H_1$) limb skeletal morphology evolved stochastically; or ($H_2$) limb skeletal morphology evolved via adaptive mechanisms to fluctuations in biome. To test these hypotheses, we took a multi-analysis approach by modeling evolutionary mode (pattern of evolution), and evolutionary tempo (rate of evolution among biomes), as well as plotting disparity through time to visualize the interaction between tempo and mode.

Variation in selective pressures among biomes can result in differing rates of phenotypic evolution among populations (Hendry et al., 2008; Kinnison & Hendry, 2001). During the Pleistocene, such variation in selective pressures could be tied to the expansion of novel niche space as glaciers retreated, with populations expanding into these habitats and subsequently exhibiting faster rates of evolution. In addition, populations undergoing adaptation to novel biomes often present with a loss of morphological disparity through time as selection culls the extreme phenotypes from a population (Foote, 1997; Schluter, 2000; Slater,

Price, Santini, & Alfaro, 2010). For this study, we quantified limb shape using 3D geometric morphometric landmark data and size using centroid size from 24 specimens of *M. americana* and *M. caurina* that were sequenced and included in a previously constructed Bayesian phylogeny (Figure 2; Lynch, 2019a). We chose to study limbs because there is a correlation between limb shape, locomotor mode, and environment in Carnivora (Fabre et al., 2015; Fabre, Cornette, Slater, et al., 2013; Kilbourne, 2017; Polly, 2008, 2010). Martens shift their predominant locomotor patterns in response to vegetation density and type, and, therefore, the limbs provide a relatively direct interface between environmental selective pressures and the morphology these pressures influence (Andruskiw, Fryxell, Thompson, & Baker, 2008; Fuller & Harrison, 2005; Moriarty et al., 2015; Steventon & Major, 1982). Previous research has demonstrated that limb shape and proportions differ among marten populations from different biomes and within different climates (Lynch, 2019b). Within coniferous forest biomes, martens exhibit very robust limb morphologies with proportionally larger olecranon processes, elongated distal epiphyses on the radius, broad tibial plateaus, and enlarged fibular heads. This is in contrast to the gracile morphologies of martens from broadleaf forest biomes. Limb proportions were found to correlate with annual temperature and precipitation, with individuals living in colder, wetter regions having longer limbs. If the limb skeletal morphology of North American *Martes* evolved as an adaptation to biome, we predict that: (a) limb skeleton shape and/or size changes will reflect non-stochastic modes of evolution (e.g., Ornstein-Uhlenbeck); (b) rates of evolution will significantly differ among specimens from different biomes (but not necessarily different species), with individuals from boreal and/or broadleaf forest exhibiting faster rates as these biomes shifted the most at the end of the Pleistocene (Jackson et al., 2000); and (c) intra-clade disparity will increase and decrease in conjunction with available geographic ranges, reflecting the emergent pattern of glacial cycles.

We analyze the tempo and mode at which limb elements accrue variation using multiple individuals representing genetically discrete populations of *M. americana* and *M. caurina*. By examining these shifts between the two species via evaluation of individuals from geographically disconnected populations, we aimed to capture intraspecific variation that reflects temporal scales of adaptive divergence and ecological speciation. Phylogenetic comparative evolutionary modeling is often conducted to evaluate the accumulation of variation in traits as measured by the underlying phylogeny (e.g., Law, 2019; Law et al., 2018a; Rüber & Adams, 2001; Slater et al., 2010; Weber, Mitko, Eltz, & Ramírez, 2016), whether the tree represents species, populations or individuals (Paradis, 2015). We leverage phylogeny-based comparative methods to evaluate the evolution of limb shape and size across North American *Martes*, treating genetically distinctive lineages as clades representative of population divergence and historical biogeography. We also ran each analysis for each species and biome independently, but found these results did not differ considerably from those obtained for the full clade (Supplemental S1, Section D).

### 1.1 | Taxonomic nomenclature

North American pine martens, *M. americana* and *M. caurina*, were recently proposed as unique species based on mitochondrial, nuclear, morphological, and parasitological evidence (Dawson et al., 2017; Dawson & Cook, 2012; Hoberg, Koehler, & Cook, 2012; Lynch, 2019a; Merriam, 1890), but have not yet been recognized by the International Commission on Zoological Nomenclature. Nonetheless, we have adopted these recommended titles throughout this manuscript.

### 1.2 | Institutional abbreviations

New York State Museum (NYSM), Florida Museum of Natural History (FLMNH), Museum of Southwestern Biology (MSB), Burke Museum of Natural History and Culture (BMUW), University of Alaska Museum of the North (UAMN), Smithsonian Institution National Museum of Natural History (USNM).

## 2 | MATERIALS AND METHODS

### 2.1 | Specimens

We measured the appendicular skeletal morphology of 24 individuals genetically identified as *M. americana* and *M. caurina* (Supplemental S1, Section A). This data set comprised 20 specimens of *M. americana* and 4 specimens of *M. caurina*. These individuals represent 24 of the 80 specimens included in a previously constructed Bayesian phylogeny (Figure 2; Lynch, 2019a). All measured specimens were adults as determined by complete epiphyseal fusion. Both sexes were included in this study with 14 males, 7 females, and 3 of unknown sex (Supplemental S1, Section A). Sexual dimorphism has been reported in the cranial morphology and body size of these species, however, to date there have been no studies assessing the degree of dimorphism in skeletal limb morphology (Clark et al., 1987; Colella, Johnson, & Cook, 2018; Nowak, 1999). We, therefore, tested for dimorphism within our data set as means of better interpreting the evolutionary tempo and mode of skeletal limb morphology.

We found significant differences in the centroid size of the femur and fibula between sexes (see Supplemental S1, Section B for methods and results). Specimens were collected across the U.S. range of these species between 1990 and 2013 (Figure 2). We assigned each specimen to one of three biomes based on the geographic location from which it was collected: (a) temperate broadleaf and mixed forest ($N = 9$; all *M. americana*); (b) temperate coniferous forest ($N = 5$; majority [$N = 4$] *M. caurina*); and (c) boreal forest ($N = 10$; all *M. americana*) (Olson et al., 2001). By sampling from each of the biomes occupied by these species, we aimed to capture the full range of morphological variation present in *M. americana* and *M. caurina*. These specimens are housed in the collections at NYSM, FLMNH, MSB, BMUW, UAMN, and USNM. Because these species actively hybridize where their ranges overlap in the western U.S. and Canada, and because hybrids exhibit a different morphology than either species (Colella, Johnson, & Cook, 2018), we chose to exclude specimens collected from these regions so as not to confound our evolutionary signal. In addition, it is important to note that there is a paucity of postcranial elements in museum collections for commercially valuable furbearers, as distal limb elements are often removed and/or preserved with skins. Due to this factor, our sample sizes are necessarily low; we, therefore, use permutational, Bayesian, and small-sample-size-appropriate methodologies wherever possible throughout our analyses.

## 2.2 | Bayesian phylogeny

To provide a phylogenetic framework for comparative analysis, we used a previously constructed phylogeny (Lynch, 2019a) containing the same individuals whose skeletal limb morphologies were measured. The phylogeny was created using sequences of the cytochrome b (cytb) mitochondrial gene and was time-calibrated using three fossil occurrence date ranges at three nodes: the divergence between the ingroup and outgroup clades (5.33–1.75 Mya); the node for crown *M. americana* (126–11.7 kya); and the node for crown *M. caurina* (1.8 Mya-11.7 kya). For a description of priors, phylogeny construction, and topological interpretation see Lynch (2019a).

## 2.3 | Appendicular skeletal morphology

We collected shape data from six appendicular skeletal elements (humerus, radius, ulna, femur, tibia, and fibula) of 24 individuals. We collected 3D geometric morphometric landmark data from each bone using a MicroScribe G2LX digitizer, which records the X, Y, and Z coordinates of a single point/landmark in space. We chose landmarks that would best capture the length and width of each element (Figure 3; Table 1; following for example, Meachen-Samuels & Van Valkenburgh, 2009; Fabre, Cornette, Peigné, & Goswami, 2013; Samuels et al., 2013; Meachen, Dunn, & Werdelin, 2015). In order to potentially capture phylogenetic signal within limb shape, we chose landmarks that represented morphological characters frequently used in phylogenetic studies of carnivorans (Figure 3; Table 1; Leach, 1977; Zrzavý & Řičánková, 2004; Morlo & Peigné, 2010; Meachen-Samuels, 2012). We also chose landmarks that have been shown to reflect locomotor variation in mustelids (Fabre et al., 2015; Fabre, Cornette, Peigné, & Goswami, 2013; Fabre, Cornette, Slater, et al., 2013) and that have successfully differentiated specimens of North American *Martes* from different biomes (Lynch, 2019b). Landmarks were aligned for each bone independently using a series of generalized Procrustes analyses (GPA; i.e., one GPA one for each limb element), and then the centroid size of each element was calculated for every specimen (all raw

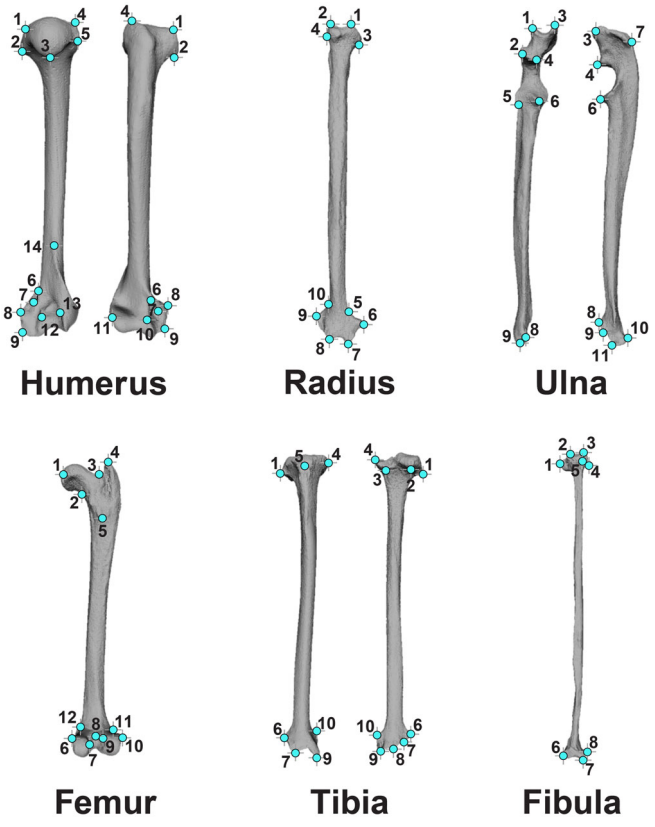


**FIGURE 3** Geometric morphometric landmarks on the humerus, radius, ulna, femur, tibia, and fibula used to quantify bone shape of specimens (from Lynch, 2019b). These landmarks have been shown to successfully capture bone shape and differentiate specimens from different biomes (Lynch, 2019b). See Table 1 for landmark definitions

**TABLE 1** Geometric morphometric landmark definitions from Lynch (2019b)

| Element | Landmark | Description |
|---|---|---|
| **Humerus** | 1 | Most superior point of the lesser tubercle |
| | 2 | Most inferomedial point of the lesser tubercle |
| | 3 | Most inferior point of the head |
| | 4 | Most superior point of the greater tubercle |
| | 5 | Most inferior and medial point on the greater tubercle |
| | 6 | Most superior point within the entepicondylar foramen |
| | 7 | Most inferior point within the entepicondylar foramen |
| | 8 | Most superior point of the medial epicondyle |
| | 9 | Most inferior point of the medial epicondyle |
| | 10 | Most medial intersection of the trochlea and coronoid fossa |
| | 11 | Most lateral intersection of the trochlea and coronoid fossa |
| | 12 | Most medial intersection of the trochlea and olecranon fossa |
| | 13 | Most lateral intersection of the trochlea and olecranon fossa |
| | 14 | Most superior point of the lateral supracondylar ridge |
| **Radius** | 1 | Most superior point on the anterior surface of the articular circumference of the head of the radius |
| | 2 | Most superior point on the posterior surface of the articular circumference of the head of the radius |
| | 3 | Most inferomedial point at the intersection of the articular circumference and neck |
| | 4 | Most inferolateral point at the intersection of the articular circumference and neck |
| | 5 | Point of maximum curvature of the medial intersection of the trochlea and body |
| | 6 | Most medial point of the ulnar notch |
| | 7 | Most inferior point of the styloid process |
| | 8 | Most inferior point of the trochlea lateral to the styloid process |
| | 9 | Most lateral point of the trochlea opposite the ulnar notch |
| | 10 | Point of maximum curvature of the lateral intersection of the trochlea and body |
| **Ulna** | 1 | Most superolateral point of the proximal tuberosity of the olecranon |
| | 2 | Most anterolateral point of the cranial process of the trochlear notch |
| | 3 | Most superomedial point of the proximal tuberosity of the olecranon |
| | 4 | Most anteromedial point of the cranial process of the trochlear notch |
| | 5 | Most anterior point of the craniolateral process of the trochlear notch |
| | 6 | Most anterior point of the craniomedial process of the trochlear notch |
| | 7 | Most inferoposterior point of the proximal tuberosity of the olecranon |
| | 8 | Most superior point of the articular surface that articulates with the ulnar notch of the radius |
| | 9 | Most inferior point of the articular surface that articulates with the ulnar notch of the radius |
| | 10 | Most posterior point of the styloid process just superior to the insertion point of the carpi ulnaris muscle |
| | 11 | Most anterior point of the styloid process just superior to the insertion point of the carpi ulnaris muscle |
| **Femur** | 1 | Center of the fovea capitis |
| | 2 | Point of maximum curvature of the neck of the femur along the coronal plane |
| | 3 | Point of maximum curvature between the femoral head and greater trochanter along the coronal plane |

(Continues)

**TABLE 1** (Continued)

| Element | Landmark | Description |
|---|---|---|
| | 4 | Most superior point of the greater trochanter |
| | 5 | Most inferoposterior point of the lesser trochanter |
| | 6 | Most superomedial point of the medial condyle |
| | 7 | Most superolateral point of the medial condyle |
| | 8 | Most superior point of the intercondylar fossa along the sagittal plane |
| | 9 | Most superomedial point of the lateral condyle |
| | 10 | Most superolateral point of the lateral condyle |
| | 11 | Most anterior point of the lateral sesamoid facet |
| | 12 | Most anterior point of the medial sesamoid facet |
| **Tibia** | 1 | Most lateral point of the lateral condyle |
| | 2 | Most inferoposterior point of the lateral condyle |
| | 3 | Most inferoposterior point of the medial condyle |
| | 4 | Most medial point of the medial condyle |
| | 5 | Most anterior point along the sagittal plane of the tibial tuberosity |
| | 6 | Most superolateral point of the lateral malleolus |
| | 7 | Most inferior point of the lateral malleolus |
| | 8 | Most inferoposterior point of the distal epiphysis that is not part of the medial or lateral malleolus |
| | 9 | Most inferior point of the medial malleolus |
| | 10 | Most superomedial point of the medial malleolus |
| **Fibula** | 1 | Most anterior point of the head |
| | 2 | Most superior point of the head anterior to the coronal plane |
| | 3 | Most superior point of the head posterior to the coronal plane |
| | 4 | Most posterior point of the head |
| | 5 | Most medial point of the head along the coronal plane |
| | 6 | Most anterior point of the lateral malleolus |
| | 7 | Most inferior point of the malleolar articular surface |
| | 8 | Most posterior point of the distal epiphysis lateral to the malleolar articular surface |

data and R code is available via figshare DOI: 10.6084/m9.figshare.9864146). We used centroid size values to represent bone size in further analyses. All tests were performed using the geomorph package (Adams, Collyer, Kaliontzopoulou, & Sherratt, 2017) in R (R Core Team, 2015). Previous research indicates very weak allometric relationships between bone shape and centroid size, with only 3–6% of shape variation attributable to size (Lynch, 2019b). We, therefore, did not allometrically-correct our shape data.

## 2.4 | Evolutionary mode

We evaluated the mode of variance accumulation in limb element sizes using centroid size by comparing the following models: Brownian motion (random walk; Felsenstein, 1973), Ornstein-Uhlenbeck (adaptive-peak; Butler & King, 2004), lambda (independent evolution; Pagel, 1999), kappa (punctuated; Pagel, 1999), Δ(time-dependent; Pagel, 1999), and early burst (accellerating-decelerating; Blomberg, Garland Jr, Ives, & Crespi, 2003; Harmon et al., 2010). The goodness-of-fit of these evolutionary models was evaluated using both log-likelihood and AICc values. We also calculated ΔAICc to determine if any models were equally good fits, with a ΔAICc of 2 as our threshold (Burnham & Anderson, 2002; Burnham & Anderson, 2004). These analyses were run in R (R Core Team, 2015) using the ape (Paradis, Claude, & Strimmer, 2004), GEIGER (Harmon, Weir, Brock, Glor, & Challenger, 2008), and phytools (Revell, 2012) packages (figshare DOI: 10.6084/m9.figshare.9864146). We then

transformed the phylogeny according to the best-fit model of evolution and the resulting tree was used in subsequent analyses of phylogenetic signal and differences in evolutionary rate.

We then identified the best-fit evolutionary mode for limb element shape for each element independently. To reduce the dimensionality of the landmark data, we quantified shape using Principal Component scores that describe the first 95% of variation within the data set. We fit five evolutionary models: Brownian motion (random walk; Felsenstein, 1973), Ornstein-Uhlenbeck (adaptive-peak; Butler & King, 2004), lambda (independent evolution; Pagel, 1999), kappa (punctuated; Pagel, 1999), Δ(time-dependent; Pagel, 1999), and early burst (accellerating-decelerating; Blomberg et al., 2003; Harmon et al., 2010). These analyses were run in BayesTraitsV3 (http://www.evolution.rdg.ac.uk/; Pagel & Meade, 2006) using a reversible jump Markov Chain Monte Carlo algorithm and allowing for variable rates of evolution along each branch and node (Varrates). We ran each analysis for 100,000,000 iterations with a burnin of 12,500,000. We calculated goodness of fit using the marginal likelihood of each model, which was estimated using steppingstone sampling. We then compared the evolutionary models using Bayes Factor to determine which best fit the shape data. The Bayes Factor was calculated using the BTRtools package (https://github.com/hferg/btrtools) in R (R Core Team, 2015) (figshare DOI: 10.6084/m9.figshare.9864146). For each element, we calculated the mean tree for the best-fit model for use in subsequent analyses of phylogenetic signal and evolutionary rate.

## 2.5 | Phylogenetic signal

We calculated phylogenetic signal for limb skeletal shape within the centroid size (univariate) and GPA aligned landmark data (multivariate) within each limb, independently. This allowed us to determine whether the limb skeletal morphology of closely related individuals of *M. americana* and *M. caurina* are statistically dependent on phylogenetic structure. First, we estimated phylogenetic signal for centroid size using two indices and their associated significance tests: Blomberg's K (Blomberg et al., 2003) and Pagel's λ (Pagel, 1999). We estimated the significance of values returned for Blomberg's K using a permutation method set to 999 iterations (Blomberg et al., 2003). For Pagel's λ, significance was determined by incorporation of sampling error, after Ives, Midford, and Garland Jr (2007). We calculated both indices as a means of comparing to the results of the multivariate extension of Blomberg's K ($K_{mult}$) analysis (described below), and because Pagel's λ is a more accurate measure of phylogenetic signal in phylogenies with few tips (Münkemüller et al., 2012). We ran these analyses in R (R Core Team, 2015) using the phytools package (Revell, 2012) (figshare DOI: 10.6084/m9.figshare.9864146).

Second, we estimated phylogenetic signal within the landmark data through a generalization of Blomberg's K (Blomberg et al., 2003) that is more appropriate for multivariate data ($K_{mult}$) (Adams, 2014b; Adams & Collyer, 2018). This model is ideal for geometric morphometric data because it has high statistical power and appropriate Type I error ($\alpha = .05$) even with high trait dimensionality and covariance (Adams, 2014a; Adams & Collyer, 2018). We ran this analysis in R (R Core Team, 2015) using the geomorph package and the function "physignal" (Adams et al., 2017) (figshare DOI: 10.6084/m9.figshare.9864146).

## 2.6 | Evolutionary rate

We tested for differences in the rate at which limb elements accrued variation (tempo) among specimens from the three biomes occupied by North American *Martes*: (a) temperate broadleaf and mixed forest; (b) temperate coniferous forest; and (c) boreal forest (Olson et al., 2001). For this analysis, we quantified limb bone size using the centroid sizes of each

**TABLE 2** Mode of evolution for limb element centroid size

| | Limb element | | | | | | | | | | | |
|---|---|---|---|---|---|---|---|---|---|---|---|---|
| | Humerus | | Radius | | Ulna | | Femur | | Tibia | | Fibula | |
| Model | Log-like | AICc | Log-like | AICc | Log-like | AICc | Log-like | AICc | Log-like | AICc | Log-like | AICc |
| Kappa | −151.89 | 308.39 | −141.81 | 288.23 | −148.56 | 301.71 | −159.39 | 323.37 | −156.72 | 318.05 | −160.49 | 325.59 |
| OU | −161.60 | 327.80 | −142.61 | 289.82 | −161.82 | 328.24 | −172.62 | 349.83 | −161.73 | 328.06 | −159.32 | 323.24 |
| BM | −161.67 | 325.53 | −148.34 | 298.86 | −163.66 | 329.50 | −177.33 | 356.84 | −171.90 | 346.00 | −170.26 | 342.71 |
| Delta | −158.50 | 321.61 | −143.72 | 292.05 | −162.93 | 330.46 | −170.61 | 345.81 | −163.34 | 331.28 | −163.32 | 331.23 |
| EB | −164.20 | 332.99 | −145.34 | 295.28 | −164.96 | 334.53 | −175.16 | 354.92 | −170.22 | 345.04 | −169.32 | 343.24 |

Abbreviations: BM, Brownian Motion; EB, Early Burst; OU, Ornstein-Uhlenbeck.

element, and calculated evolutionary rates from these data iteratively for each element ("compare.evol.rates" function in the geomorph package (Adams et al., 2017)). Evolutionary rates were calculated by phylogenetically transforming the shape data under a BM null model of evolution and then calculating the resulting between-specimen Euclidian distances. Rate is then quantified as the sum of squared distances between the phylogenetically transformed data and the origin of the phylogeny (Adams, 2014b). We then compared ratios of rates between each biome to ratios of rates produced from simulated data with rates that do not significantly differ using a simulation method with 999 iterations (after Denton & Adams, 2015). This analysis produces appropriate type I error and high power, despite small rate differences between groups (Adams & Collyer, 2018).

We also tested for differences in evolutionary rate of overall limb bone shape changes among the three different biomes using 3D landmark data and the "compare.evol.rates" function in the geomorph package, evaluating significance using the permutation method with 999 iterations (Adams et al., 2017).

We replicated these evolutionary rate comparisons of centroid size and landmark data using species as the grouping factor to determine whether *M. americana* or *M. caurina* were evolving at different rates. We ran all analyses in R (R Core Team, 2015) using the geomorph package (Adams et al., 2017) (figshare DOI: 10.6084/m9.figshare.9864146).

## 2.7 | Morphological disparity

We modeled morphological disparity through time in *Martes* from the Pleistocene to the Present following quantification of bone shape (3D landmark data) and centroid size using the "dtt" function in the GEIGER package (Harmon et al., 2008) (figshare DOI: 10.6084/m9.figshare.9864146). We used the original time-calibrated Bayesian phylogeny and chose an average squared Euclidian distance disparity index as indicated for geometric morphometric analyses (Zelditch, Swiderski, & Sheets, 2012) and small sample sizes (Ciampaglio, Kemp, & McShea, 2001). We then compared the estimated disparity through time to that expected under a BM null model of evolution using the morphological

**TABLE 3** Kappa values for limb element centroid size

| Element | Kappa |
|---|---|
| Humerus | 0.065 |
| Radius | 0.120 |
| Ulna | 0.033 |
| Femur | 0.000 |
| Tibia | 0.134 |
| Fibula | 0.000 |

**TABLE 5** Lambda values for limb element shape

| Element | Lambda |
|---|---|
| Humerus | 0.16 |
| Radius | 0.04 |
| Ulna | 0.07 |
| Femur | 0.15 |
| Tibia | 0.06 |
| Fibula | 0.11 |

**TABLE 6** Phylogenetic signal in limb element centroid size and shape

| Element | Kmult | Kmult *p* | K | K *p* | λ |
|---|---|---|---|---|---|
| Humerus | 0.96 | 0.28 | 0.38 | 0.25 | <0.01 |
| Radius | *1.00* | *<0.01* | 0.31 | 0.48 | <0.01 |
| Ulna | *1.00* | *0.02* | 0.44 | 0.12 | 0.42 |
| Femur | 0.91 | 0.23 | 0.38 | 0.35 | <0.01 |
| Tibia | 0.96 | 0.08 | 0.36 | 0.20 | <0.01 |
| Fibula | *0.95* | *0.05* | 0.16 | 0.15 | <0.01 |

All p-values less than 0.05 were considered significant.

**TABLE 4** Marginal log-likelihoods for mode of evolution for limb element shape

| | Limb element | | | | | |
|---|---|---|---|---|---|---|
| Model | Humerus | Radius | Ulna | Femur | Tibia | Fibula |
| Kappa | 1,050.17 | 941.74 | 952.68 | 1,169.56 | 1,061.78 | 934.63 |
| OU | 1,107.49 | 966.10 | 982.92 | 1,147.78 | 1,082.48 | 910.67 |
| BM | 799.09 | 748.69 | 747.30 | 895.91 | 837.49 | 724.43 |
| Delta | 998.46 | 971.27 | 963.73 | 1,144.54 | 1,063.65 | 908.96 |
| Lambda | 1,104.50 | 1,048.94 | 1,048.85 | 1,241.25 | 1,159.73 | 977.22 |

Abbreviations: BM, Brownian Motion; OU, Ornstein-Uhlenbeck.

*Note:* Grey cells indicate the evolutionary model supported by Bayes Factor.

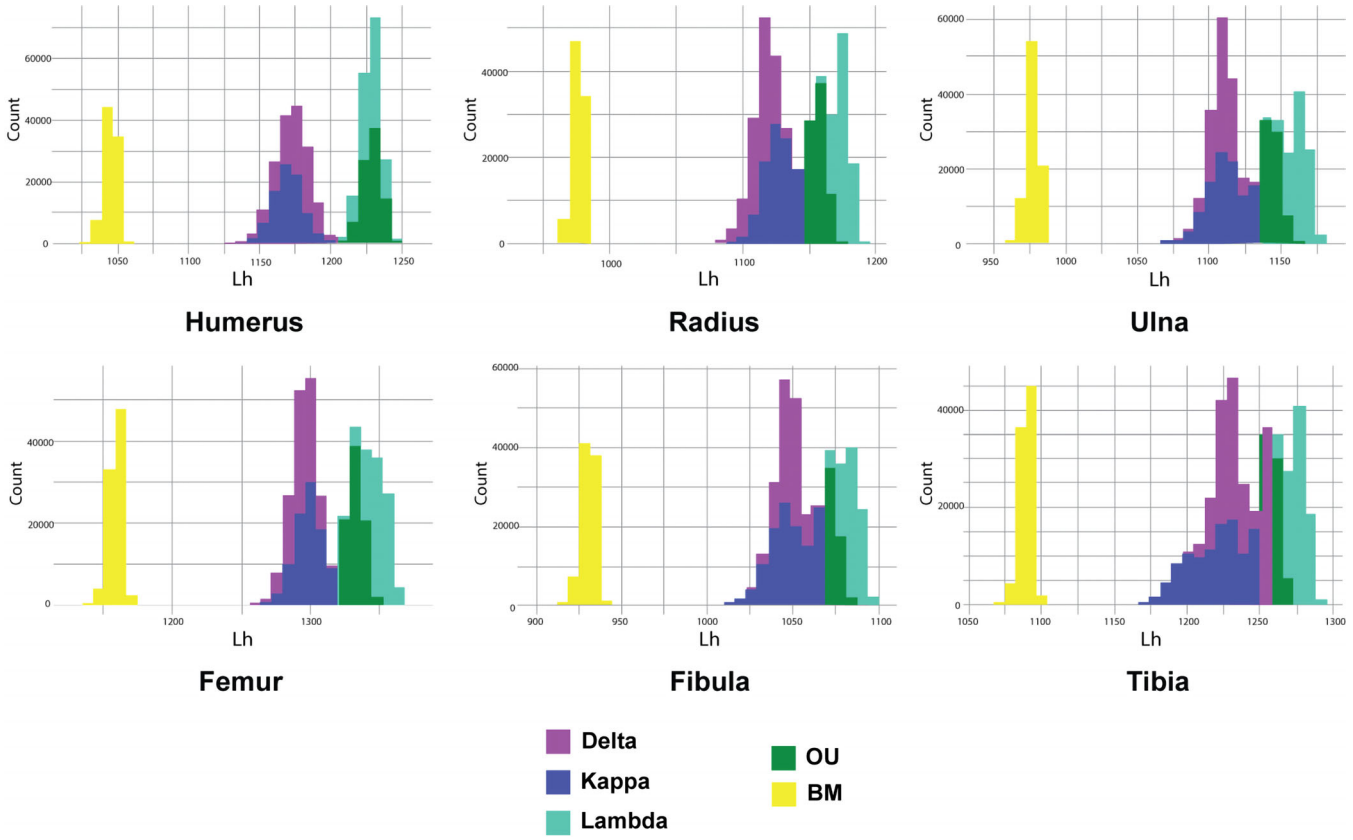


**FIGURE 4** Posterior probability distribution curves of the log likelihood value for each of the tested evolutionary models (delta, kappa, lambda, OU, BM) for limb element shape. An overlap in model distributions suggests a similar goodness-of-fit. Marginal likelihood values in Table 4 indicate which of these models was determined to be the best fit

**TABLE 7** Tempo of evolution by biome for limb element centroid size

| | | Evolutionary rates by biome | | |
|---|---|---|---|---|
| **Element** | ***p*** | **Boreal Forest** | **Broadleaf Forest** | **Coniferous Forest** |
| Humerus | .57 | 55.22 | 40.59 | 25.54 |
| Radius | .89 | 40.40 | 26.81 | 31.18 |
| Ulna | .99 | 30.78 | 31.42 | 30.46 |
| Femur | .38 | 58.81 | 37.34 | 20.38 |
| Tibia | .93 | 71.51 | 61.78 | 53.03 |
| Fibula | *.02* | *5,723.96* | *1956.00* | *593.07* |

All p-values less than 0.05 were considered significant.

**TABLE 8** Tempo of evolution by biome for limb element shape

| | | Evolutionary rates by biome | | |
|---|---|---|---|---|
| **Element** | ***p*** | **Boreal forest** | **Broadleaf forest** | **Coniferous forest** |
| Humerus | .55 | 6.52 | 8.14 | 5.94 |
| Radius | .84 | 15.67 | 17.93 | 16.32 |
| Ulna | .81 | 10.89 | 12.51 | 10.92 |
| Femur | .68 | 12.29 | 10.69 | 12.38 |
| Tibia | *.02* | *10.31* | *13.27* | *7.00* |
| Fibula | .10 | 13.22 | 21.24 | 13.78 |

All p-values less than 0.05 were considered significant.

**TABLE 9** Tempo of evolution by species for limb element centroid size

| | | Evolutionary rates by species | |
|---|---|---|---|
| **Element** | ***p*** | ***M. americana*** | ***M. caurina*** |
| Humerus | .27 | 48.38 | 19.41 |
| Radius | .61 | 35.44 | 23.11 |
| Ulna | .64 | 32.62 | 22.64 |
| Femur | .15 | 48.60 | 13.51 |
| Tibia | .48 | 69.01 | 39.01 |
| Fibula | *.04* | *3,790.29* | *500.78* |

**TABLE 10** Tempo of Evolution by Species for Limb Element Shape

| | | Evolutionary rates by species | |
|---|---|---|---|
| **Element** | ***p*** | ***M. americana*** | ***M. caurina*** |
| Humerus | .71 | 7.15 | 6.29 |
| Radius | .77 | 16.83 | 15.76 |
| Ulna | .92 | 11.55 | 11.31 |
| Femur | .27 | 11.29 | 13.80 |
| Tibia | .08 | 11.40 | 7.39 |
| Fibula | .58 | 16.75 | 14.32 |

disparity index (MDI). To calculate MDI, we simulated centroid size evolution under a BM null model of evolution 1,000 times. From these simulated data the mean relative disparity at each node is generated.

## 3 | RESULTS

### 3.1 | Evolutionary mode

We found the best-fit evolutionary model for centroid size, based on log-likelihood AICc, and ΔAICc scores, was kappa (punctuated) for all the limb elements except the radius and fibula (Table 2). The best fit models for the radius, based on log-likelihood and AICc values was kappa, however ΔAICc indicated that OU (adaptive peak) was an equally good fit. The best-fit model for the fibula was OU, with kappa as the second best-fit. Kappa values for the elements ranged from 0.0 to 0.13 (Table 3), indicating that appendicular size evolution is occurring predominantly at the tree nodes (points of genetic divergence). In all six elements, lambda could not be tested for goodness-of-fit because transformation of the phylogeny under this model results in zero-length branches.

The Bayes Factor values indicated that the best-fit evolutionary model for limb element shape was lambda for all of the elements except the humerus, which had a best-fit model of OU and a second best-fit of lambda (Table 4). Mean lambda values for each element ranged from 0.04 to 0.16 (Table 5). The posterior distribution of log likelihood values for each evolutionary model shows that for each element there is considerable overlap between lambda and OU models, suggesting limb shape may have evolved following either model (Figure 4).

### 3.2 | Phylogenetic signal

We found no phylogenetic signal in the centroid size of five of the measured elements (Table 5). There was moderate signal in the ulna, with Blomberg's K being not significant but λ equaling 0.42. We found that there was significant phylogenetic signal ($p \leq .05$) in the landmark data in the radius, ulna, and fibula (Table 5). The remaining elements did not have significant phylogenetic signal values for the multivariate landmarks.

### 3.3 | Evolutionary rate

We found that there was a significant difference in rates of evolution among the centroid size of individuals from broadleaf, boreal, and coniferous forest biomes within the fibula ($p < .05$, Table 7). Individuals from boreal forest biomes had significantly faster rates of fibular centroid size evolution. There was no significant difference in rates of centroid size evolution among the other five elements. We found a significant difference in the rate of evolution of tibial element shape among specimens collected from the three different biomes ($p < .05$, Table 8), with individuals from broadleaf forests exhibiting the fastest rate of evolution. There was no difference in evolutionary rates for shape changes in the other five measured elements. When compared directly, element specific evolutionary rates calculated with respect to biome are 2.7–433 times faster for size than for shape (Tables 7 and 8).

We also found a significant ($p < .05$) difference in the evolutionary rates of centroid size in the fibula between *M. americana* and *M. caurina* (Table 9). There was no difference in centroid size evolutionary rates in the other five elements, nor were there significant differences in rates of evolution between species in limb element shape (Table 10). Importantly, however, nearly all rates were higher for *M. americana* compared to *M. caurina*: 1.5–7.6 times higher for size and 1.02 to 1.5 times higher for shape (with the exception of the femur, which has a 20% lower rate in *M. americana*; Tables 9 and 10). Similar to the rates calculated from biome, variance in size shifts more rapidly than variance in shape (Tables 9 and 10).

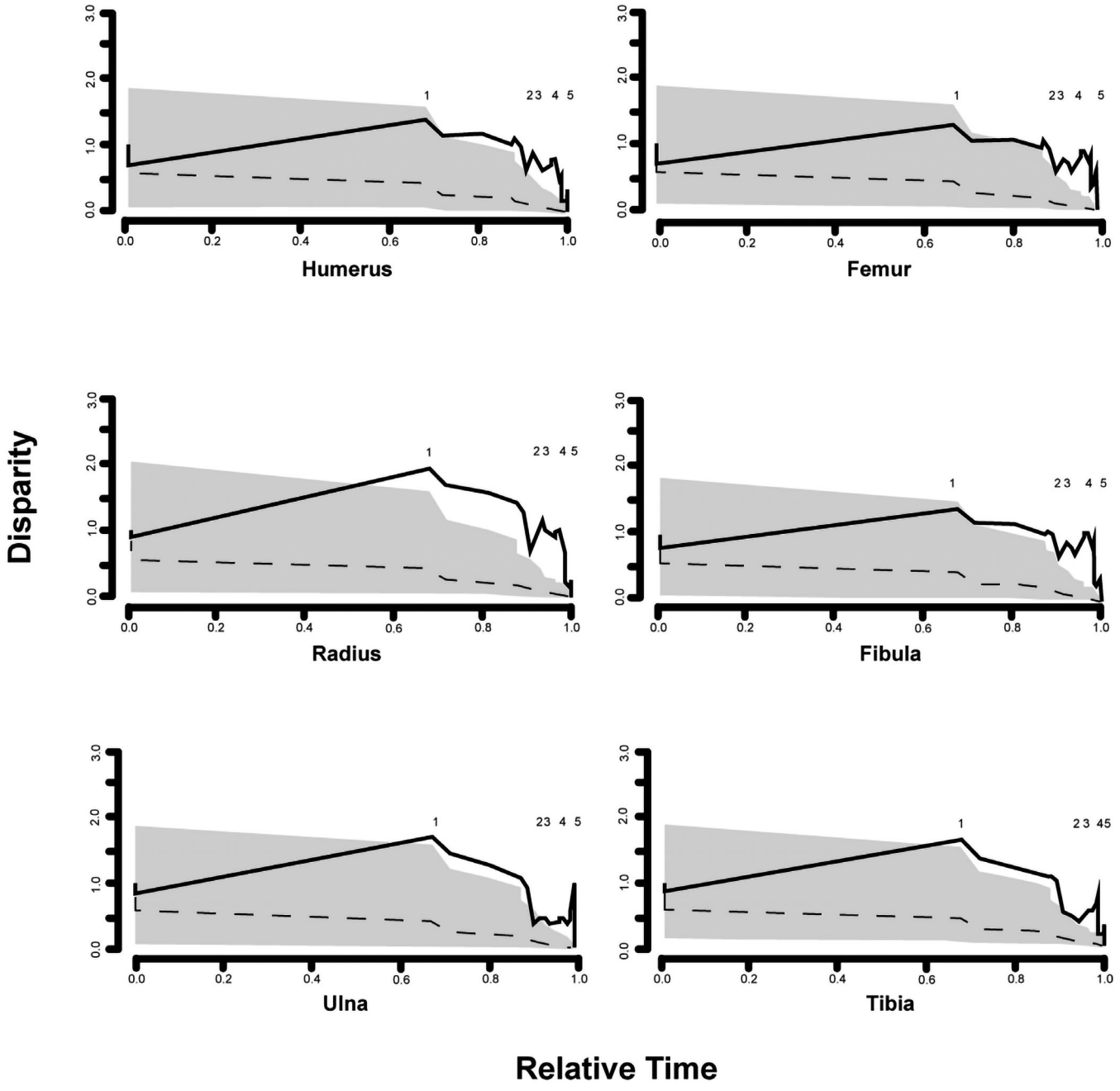


**FIGURE 5** Disparity through time (DTT) plots for the centroid size of the humerus, radius, ulna, femur, fibula, and tibia. Solid lines on the DTT plot represent estimates of the mean subclade morphological disparity. The dotted black line is the simulated disparity calculated under a Brownian motion null model of evolution with 95% confidence intervals in grey. The x-axis on each plot indicates the relative time since the basal node divergence. Numbers 1–5 within each plot reference valleys or peaks in disparity that are consistent among the six limb elements and that coincide with periods of glaciation or climatic fluctuations

## 3.4 | Morphological disparity

While the dtt plots depict relative time, it is possible to correlate ages of peaks and valleys based on the underlying phylogeny (Figure 1; Lynch, 2019a). In the centroid size of all six elements, morphological disparity was estimated to have reached an initial peak approximately 177 kya (Figure 5). This peak was then followed by a declining trend, marked by an abrupt drop in disparity ~53 kya. There were then two slight increases around 44 and 18 kya. The final slight increase in disparity occurred ~3 kya. The MDI indicated that the overall

**TABLE 11** Morphological disparity index for bone elements

| Element | Shape | Centroid size |
|---|---|---|
| Humerus | 0.70 | 0.60 |
| Radius | 0.68 | 0.99 |
| Ulna | 0.75 | 0.79 |
| Femur | 0.70 | 0.56 |
| Tibia | 0.61 | 0.76 |
| Fibula | 0.64 | 0.67 |

relative disparity of the measured data were greater than expected under a BM model of evolution with intra-clade disparity being higher than inter-clade (Table 11).

The disparity of limb shape, quantified using landmark data, appears to have reached an initial peak ~177 kya. It then gradually declined with points of brief increased disparity at 69, 10, and 3 kya (Figure 6). The

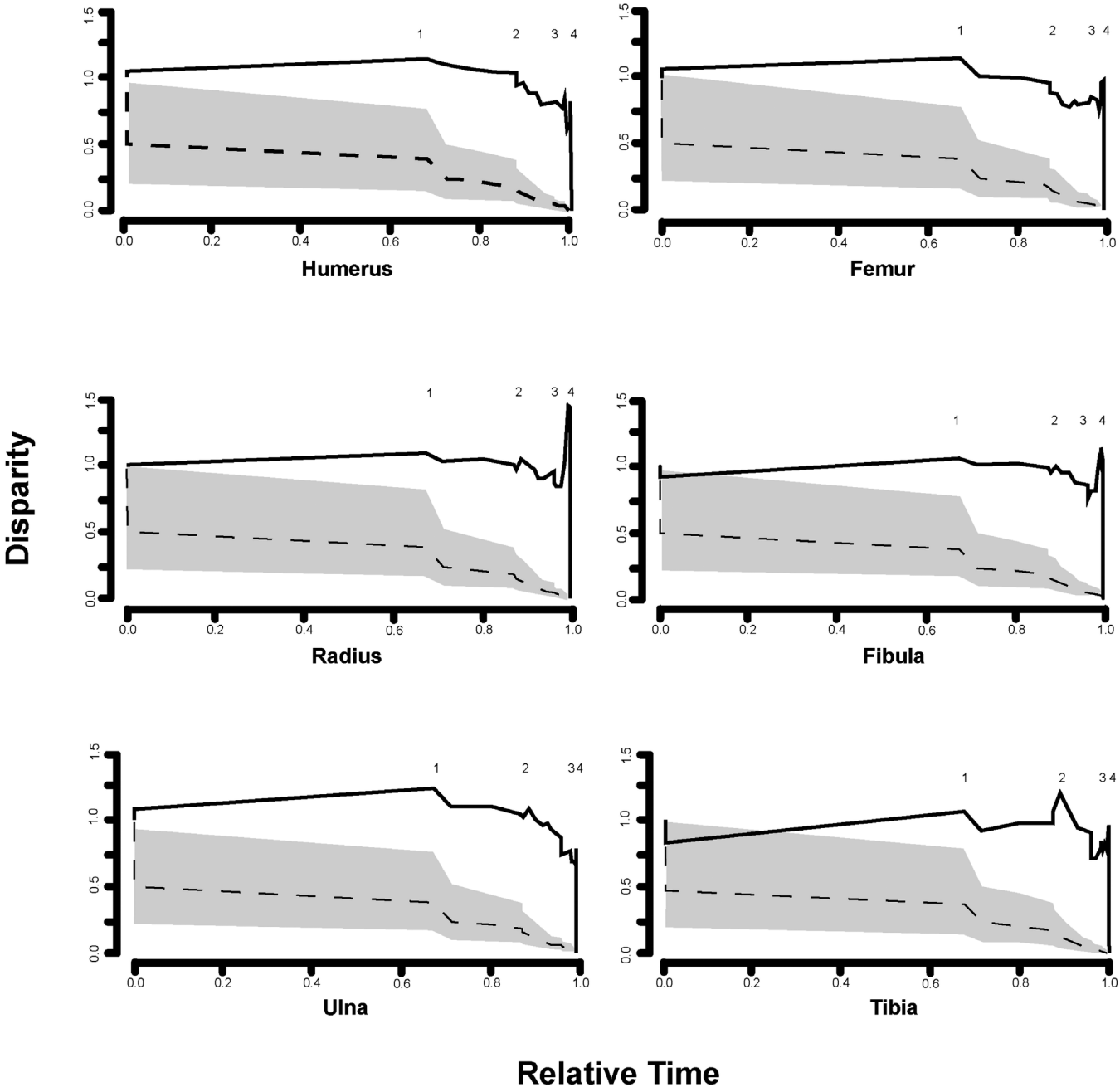


**FIGURE 6** Disparity through time (DTT) plots for shape of the humerus, radius, ulna, femur, fibula, and tibia. Solid lines on the DTT plot represent estimates of the mean subclade morphological disparity. The dotted black line is the simulated disparity calculated under a Brownian motion null model of evolution with 95% confidence intervals in grey. The x-axis on each plot indicates the relative time since the basal node divergence. Numbers 1–4 within each plot reference valleys or peaks in disparity that are consistent among the six limb elements and that coincide with periods of glaciation or climatic fluctuations

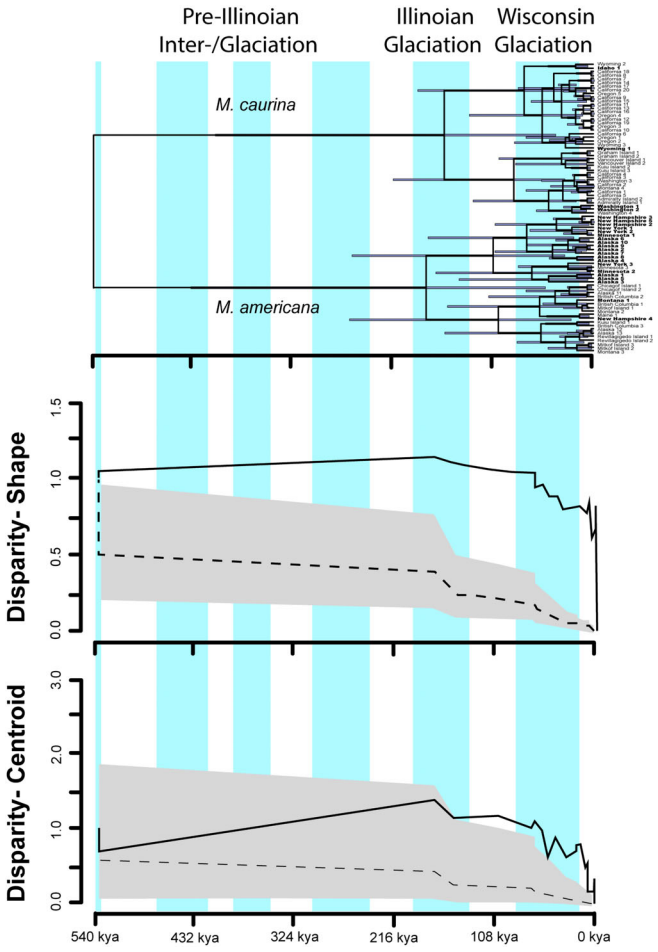


**FIGURE 7** Exemplar disparity through time (DTT) plot for the humerus with the associated time-calibrated phylogeny. The dotted black line is the simulated disparity calculated under a Brownian motion null model of evolution with 95% confidence intervals in grey. The x-axis on each plot indicates the time since the basal node divergence. Blue boxes indicate periods of glaciation, while interglacial periods remain uncolored (Folland, Karl, & Vinnikov, 1990; Ciais et al., 1992; Dyke, 2004; Lisiecki & Raymo, 2005; Clark et al., 2009; Cronin, 2010)

MDI values were all greater than zero, indicating the relative disparity was greater than would be expected under a BM null model (Table 11).

## 4 | DISCUSSION

The differing temporal scales across which evolutionary phenomena can be observed present challenges to the study of morphological trait micro- and macro-evolution (Futuyma, 2010; Hansen & Houle, 2004; Huang, 2020; Kinnison & Hendry, 2001; Li, Huang, Sukumaran, & Knowles, 2018; Voje, 2016; Wake, Roth, & Wake, 1983). Traits can change on shorter and more contemporary time scales via population-level shifts in allelic frequency, phenotypic plasticity, and adaptive divergence (Hendry et al., 2008; Kinnison & Hendry, 2001). Across longer time scales, these processes can lead to population divergence, trait fixation, and can ultimately result in ecological speciation (Hannisdal, 2006; Huang, 2020; Hunt, 2006; Hunt, Hopkins, & Lidgard, 2015; Hunt & Rabosky, 2014). Recent reviews and simulation studies underscore the need for empirical studies that span micro- and macro-evolutionary processes (Li et al., 2018; Rosindell, Harmon, & Etienne, 2015; Simons, 2002). Glacial cycles throughout the Pleistocene era represent a macrocosm of repeated ecological and evolutionary shifts that precipitated both species (longer-term) and adaptive (shorter-term) divergence. Here, we examined appendicular skeletal trait shifts in exemplar species that have evolved in concert with North American glacial cycles: *M. americana* and *M. caurina*. We map 3D geometric morphometric results for both skeletal element size and shape onto a population-level gene tree sequenced from the same 24 individuals. We then performed tree-based analyses on these geographically distinct samples, drawn from non-interbreeding populations (Colella, Johnson, & Cook, 2018; Colella, Wilson, et al., 2018; Dawson et al., 2017; Stone et al., 2002), thus comparing the two species at a deeper, speciational timescale and comparing the degree of trait variation among individuals between populations. These evolutionary analyses allowed us to measure, compare, and contrast the mode and tempo at which pine marten limb skeletal size and shape accumulate variation. We evaluated skeletal-element-specific evolutionary mode, phylogenetic signal, evolutionary rate, and disparity through time, with respect to biome and species (*M. caurina* in coniferous forests and *M. americana* in boreal and broadleaf forests). Because our sample sizes are restricted and necessarily low due to collection of furbearers, we used methods to accommodate and/or ameliorate our small and imbalanced sample sizes (e.g., permutational analysis) wherever possible. We cautiously examine our results from the perspective of within- and between-species trait divergence, mindful of decreased statistical power.

These results indicate that previously identified differences in limb size and shape of North American *Martes* arose via two different evolutionary modes, strengths of phylogenetic signal, and tempos. Limb size, as measured by centroid size, is reconstructed as having evolved through a punctuational mode of evolution, with kappa as the best supported model by AICc and log-likelihood values (Table 2). Centroid size data also has low phylogenetic signal, which is often interpreted as an adaptive signal because trait variance is less constrained by heritability (Table 6), and is often interpreted to indicate that a phenotype has evolved via a stochastic, non-

adaptive mode such as phenotypic or genetic drift (Adams, 2014a; Blomberg et al., 2003; Pagel, 1999; Revell, Harmon, & Collar, 2008). Simulations exploring the relationship between phylogenetic signal and evolutionary mode find that a punctuational mode of evolution consistently results in low phylogenetic signal, even when the strength of divergent selection is very high (Revell et al., 2008)—a pattern consistent with repeated divergence brought about by glacial/interglacial cycles. In contrast to the punctuational mode for element size, Bayes Factor values support a lambda mode of evolution for limb shape (Table 4). This lambda mode of evolution is accompanied by a high phylogenetic signal in the distal elements (Tables 4 and 6). Posterior probability distributions of log likelihood values suggest that OU may also be a good-fit for modeling limb shape evolution (Figure 4). These models, lambda and OU, indicate that shape variation is not independent of the underlying phylogenetic relationships. Therefore, the mechanisms underlying limb shape evolution would be interpreted similarly under either model.

Both the kappa/punctuational-dominant models for limb size and lambda-dominant models for limb shape indicate that changes in morphological variance are occurring in conjunction with divergence: kappa reflecting environmental-precipitated divergence for limb size, and lambda reflecting genetically-contingent divergence in limb shape. These patterns typically occur along with a mechanism of novel or shifting selective pressures (Eldredge & Gould, 1972; Flegr, 2013; Pagel, 1999). Allopatric or peripatric populations that are experiencing habitat shifting or reorganization often exemplify these modes of evolution and may even exhibit marked changes in evolutionary tempo (Hendry et al., 2008; Kinnison & Hendry, 2001).

In addition to these differences in evolutionary mode between marten limb element size and shape, the rates of trait evolution also differ between size and shape. In all cases, evolutionary rates are higher for size when compared to shape. Thus, our overall results suggest that genetic structure predicts marten limb shape better than limb size. This is congruent with broad patterns of trait evolution and development, where within- and between-element phenotypic integration constrains the response of trait shape to selection (Goswami, Binder, Meachen, & O'Keefe, 2015), although size may respond isometrically in the absence of allometric or shape change (Klingenberg, 1998).

The results of our disparity through time analyses indicate that marten limb element size and shape shifts likely occurred congruent with the expansion and contraction of North American glaciers during the Pleistocene. Differing phenotypes may arise among populations that are undergoing periods of expansion or isolation in novel environments due to shifting selective pressures (Eldredge & Gould, 1972; Gould, 2002; Mayr, 1942; Oakley, Gu, Abouheif, Patel, & Li, 2004). Glacial–interglacial cycles have been implicated with the phenotypic evolution of several clades including diatoms, birds, fishes, and mammals (e.g., Bennett, 1991; Hassanin, 2015; Lovette, 2005; Near et al., 2012; Spanbauer, Fritz, & Baker, 2018; Weir & Schluter, 2004) and likely played a key role in the evolution of *Martes*. Fossil and genetic evidence suggests that populations of *M. americana* and *M. caurina* experienced six glacial–interglacial cycles throughout the Pleistocene (1.8 Mya–11.7 kya) (Behrensmeyer & Turner, 2013; Bell et al., 2004; Eshelman & Grady, 1986; Feranec, 2009; Grady, 1984; Guilday & Hamilton, 1978; Long, 1971; Lynch, 2019a; Mead, Heaton, & Mead, 1989; Sinclair, 1907; Tankersley, 1997; Wetmore, 1962). During each of these cycles, populations would have evolved under differing selective regimes as biomes in the eastern and western U.S. underwent differing reorganization (Gill et al., 2009; Koch et al., 2004; Williams et al., 2001; Williams & Jackson, 2007). Concurrent with these changes in climate and the associated shifts in biome, overall disparity in limb morphology may have fluctuated in concert with shifting local environments. Our results identify changes in both limb size and limb shape disparity that correspond with climatic fluctuations (Figure 5). Both the disparity of limb size and shape reach a peak after the onset of the Illinoian glaciation (191–130 kya) (Cronin, 2010; Lisiecki & Raymo, 2005). During this time, these clades would have been geographically isolated within unique biomes in the eastern (boreal forests; Jackson et al., 2000; Gill et al., 2009) and western (coniferous forests; Thompson, Anderson, & Bartlein, 1999) U.S., where they would have experienced differing selective pressures. During the Wisconsin glaciation (80–11 kya) there is also considerable fluctuation in limb morphological disparity, with size and shape exhibiting different trends (Figures 5 and 7). Centroid size disparity decreases and increases several times during the Wisconsin glaciation, reaching a last peak at the end of the Last Glacial Maximum (19 kya) (Figures 5 and 7) (Clark et al., 2009; Cronin, 2010; Dyke, 2004; Lisiecki & Raymo, 2005). Limb shape disparity remained on a steady decline throughout the Wisconsin glaciation (Figures 6 and 7), not reaching its final peak until the Holocene Climatic Optimum (10–6 kya) (Ciais et al., 1992; Folland et al., 1990). Each of these periods is associated with marked changes in climate and biome.

The evolvability of a phenotype has been hypothesized to correspond with its degree of specialization (Day, Hua, & Bromham, 2016; Holmes, 1977). In the case of mammalian limb morphologies, the amount of integration

in size and shape between elements decreases with locomotor specialization (Rolian, 2019; Young & Hallgrímsson, 2005). This indicates that locomotor generalists likely have a higher limb evolvability than locomotor specialists. Mustelid species, though frequently categorized within a locomotor specialty such as fossorial, aquatic, or arboreal, all exhibit a wide range of locomotor modes. Despite many species having distinctive and dominant locomotor types, both specialist and non-specialist species appear to maintain similar degrees of limb element integration (Botton-Divet, Houssaye, Herrel, Fabre, & Cornette, 2018). This suggests that the targets of selection in mustelid locomotion are the limb girdles, such that proximal and distal limb elements are more evolutionarily labile, able to evolve toward new adaptive peaks as selective pressures shift. The results of our study suggest that North American *Martes* is no exception, with limb shape and size evolving in conjunction with genetic divergences and with Pleistocene climatic changes. Though often categorized as arboreal, *M. americana* and *M. caurina* are locomotor generalists, capable of climbing, pursuit predation, swimming, and navigating tunnel systems within the subnivium and will vary these behaviors by habitat (Andruskiw et al., 2008; Banfield, 1974; Ben-David, Flynn, & Schell, 1997; Clark et al., 1987; Fuller & Harrison, 2005; Harris & Steudel, 1997; Moriarty et al., 2015; Nowak, 1999; Steventon & Major, 1982; Zielinski & Duncan, 2004). Such locomotor generalization may be the result of higher evolvability in their limb morphologies across Pleistocene climatic and habitat fluctuations. Underscoring the argument of evolutionary lability, our results find different modes and rates of evolution between limb shape and size suggesting these features may be responding to different environmental pressures.

The independent evolution of shape and size has occurred in several other clades (e.g., Adams & Nistri, 2010; Botton-Divet et al., 2018; Friedman, Martinez, Price, & Wainwright, 2019; Law, 2019; Mitteroecker, Gunz, Bernhard, Schaefer, & Bookstein, 2004). Frequently, this independence is recognized through a lack of allometric signal and is hypothesized to act as a release from evolutionary constraints on morphology (Huxley, 1932; Simpson, 1944; Rensch, 1959; Gould, Lewontin, Smith, & Holliday, 1979; Gould, 2002; Voje, Hansen, Egset, Bolstad, & Pelabon, 2014). Previous research into the ecomorphology of North American marten limb elements has demonstrated that only 3–6% of limb shape is attributable to limb element size (Lynch, 2019b). This suggests that limb size did not act as an evolutionary constraint as limb shape evolved throughout the Pleistocene, potentially enabling North American martens to adapt to fluctuations in climate and biome quite readily. Additionally, in studies that have found little to no influence of trait size or shape, many researchers have attributed shape variation to differences in environmental selective pressures (e.g., Bol'shakov, Vasil'ev, Vasil'eva, Gorodilova, & Chibiryak, 2015; Dowle, Morgan-Richards, Brescia, & Trewick, 2015; Glennon & Cron, 2015; Abaad et al., 2016; Aguilar-Medrano & Calderon-Aguilera, 2016; Alves, Moura, & de Carvalho, 2016; Grohé, Tseng, Lebrun, Boistel, & Flynn, 2016). This pattern can be seen in our earlier studies, which have demonstrated that bone shape and size in *Martes* has previously been shown to correlate with different environmental and climatic variables (Lynch, 2019b). For example, shorter limb bones are found in individuals occupying regions with warmer annual temperatures and high amounts of precipitation, while overall limb robusticity and epiphyseal size correspond with biome and forest complexity (Lynch, 2019b). These climatic and environmental selective pressures may then have resulted in the differing evolutionary trends exhibited in limb bone size and shape.

Our previous work (Lynch, 2019b) indicates that limb size has evolved to differ with respect to climatic variables, such as temperature and precipitation. Evolutionary rates in limb size are consistently fastest in individuals from boreal forest biomes and slowest in those from coniferous forests (Tables 6). Glacial retreat at the end of the Pleistocene occurred in an easterly to westerly fashion, with that located north of the western coniferous forests being the last to retreat (Dyke, 2004) (Figure 2). As a result, Pleistocene coniferous forest biomes remained stable for a more extensive period than eastern boreal and broadleaf forests, which were undergoing reorganization into the modern biomes (Thompson et al., 1999; Jackson et al., 2000). This difference in environmental and climatic stability in the eastern and western U.S. at the end of the Pleistocene may have resulted in the differing rates of evolution seen in the limb elements of individuals from these respective biomes. In addition, around 6 kya, there was a neopluvial event in which annual precipitation increased and temperatures decreased in the western U.S. (Allison, 1982; Wilkins & Currey, 1999; Yuan, Koran, & Valdez, 2013; Noble et al., 2016; Bacon, Lancaster, Stine, Rhodes, & McCarley Holder, 2018; Adams & Rhodes, 2019). Extant populations of *Martes* from coniferous forests of the western U.S. have the longest limbs proportionally (Lynch, 2019b), suggesting that these fluctuations in temperature and precipitation influenced limb size evolution.

Limb shape, we hypothesize, evolved in response to changes in forest type. In limb shape, the fastest rates of evolution are exhibited by individuals from broadleaf forest biomes (Table 7). Limb shape in *Martes* has been shown to correlate with biome (Lynch, 2019b), suggesting that forest type has acted as a dominant selective pressure on shape evolution. This can likely be attributed to the reorganization of biomes in the eastern U.S. that

occurred at the end of the Pleistocene. As glaciers retreated, boreal forests, the dominant habitat of martens during the Pleistocene, shifted northward and were replaced by deciduous plants and eventually the broadleaf forest biome (Jackson et al., 2000). This shift in biomes then introduced changes in forest complexity, which may have in turn influenced marten behavior. Today, populations exhibit varying degrees of arboreality and different hunting strategies in correlation with forest complexity (Steventon & Major, 1982; Fuller & Harrison, 2005; Andruskiw et al., 2008; Moriarty et al., 2015). The more gracile limb morphologies seen in *M. americana* from broadleaf forests suggests that these populations were driven to more arboreal lifestyles as biomes shifted. Variation in behavior in response to climatic and biome fluctuations throughout the Pleistocene likely resulted in the differing evolutionary trends seen between limb size and shape.

The differences in the evolutionary tempo between biomes and species, as well as the differing modes of evolution seen in the tibia and fibula from the other limb elements suggest that these limb bones are under a unique set of selective pressures compared to the remaining elements. Tibia shape exhibited rates of evolution that differed among biomes, with individuals from broadleaf forests exhibiting the fastest rates (Table 4). Previous studies have shown that the proximal articulating surface of the tibia (tibial plateau) differs significantly between individuals from broadleaf and coniferous forest biomes (Lynch, 2019b), with those from broadleaf forests having a narrower plateau. Narrow tibial plateaus in small mammals correlate with higher maximum speeds as well as a more cursorial mode of locomotion (Álvarez, Ercoli, & Prevosti, 2013). The most common prey of *M. americana* are small mammals such as shrews and squirrels, but within broadleaf forests they more commonly prey on hare (*Lepus americanas*) (Buskirk, 1983; Zielinski & Duncan, 2004; Fuller & Harrison, 2005). It is possible, therefore, that selection favors faster modes of locomotion to hunt hare, acting on tibial morphology and thus resulting in the faster rates of evolution for martens inhabiting broadleaf forests. Fibula size differed in evolutionary mode as well as in rates of evolution among biomes and species. The fibula was also one of the few elements with sexually dimorphic centroid sizes. This element may be evolving toward different adaptive peaks between the sexes. It is not surprising that the tibia and fibula would simultaneously be under differing selective pressures than the other measured elements given their close anatomical association. In fact, previous research has shown that the fibular head also differs significantly among individuals from different biomes, with a more gracile morphology seen in those from broadleaf forests (Lynch, 2019b). This matches the gracile nature of the tibial plateau in broadleaf forest individuals. Future research quantifying variation in distal hindlimb morphology and its correlation with behavioral variation among biomes and between sexes may further elucidate the evolutionary history of these elements within *Martes*.

While many clades are hypothesized to have evolved in conjunction with Pleistocene glacial cycles (e.g., Zink & Dittmann, 1993; Arbogast et al., 2001; Milá et al., 2007; Shafer et al., 2010), the fossil record of these groups often is obscured by taphonomy, and phenotypic evolution must be studied from extant representatives alone—a scenario that necessarily presents an incomplete picture of phenotypic evolution. Fortunately, North American *Martes* is represented during the Pleistocene by the extinct noble marten, *M. americana nobilis*, a morphologically robust marten with a debated taxonomic status (Youngman & Schueler, 1991; Hughes, 2009; Lyman, 2011). The jaws and teeth of *M. americana nobilis* are larger in all dimensions than extant North American *Martes* and it is found in Pleistocene cave sites that implicate a mesic grassland habitat distinctive from that of the temperate and boreal habitats of extant *Martes* (Youngman & Schueler, 1991; Meyers, 2007; Hughes, 2009; Lyman, 2011). This fossil evidence suggests that the genus *Martes* was more ecologically and phenotypically diverse during the Pleistocene than extant populations would suggest. To more fully understand how the joint effects of glaciation and hybridization influenced the phenotypic evolution of North American *Martes* populations throughout the Pleistocene, future work should also assess the genotypic variation of extinct populations and include morphology from historical specimens whenever possible. By determining modes of evolution across multiple clades, including both extant and extinct populations, we can begin to better understand how communities were influenced by past climate change and thus make more informed predictions as extant populations face current climate change.

## ACKNOWLEDGMENTS

Author would like to thank A. Weil for assistance in developing and writing this research and for partial funding. Author would like to thank P. Gignac, W. Booth, N. Wilson, T. Quan for project design. Author would like to thank C. Organ for insight into methodology and interpretation. Author would like to thank J. Colella for sequences of *M. caurina*. Author would like to thank M. Belmaker, A. Watanabe, I. Browne, and H. Woodward for access to digitizers, surface scanners, and conducting photogrammetry. Thanks to S. Wallace (ETMNH), J. Dunnum (MSB), C. Thompson (UMMZ), J. Bopp (NYSM), B. Coyner (SNOMNH), A. Gunderson (UAMN), S. Peurach (USNM), V. Mathis (FMNH), and J. Bradley

(BMUW) for access to collections and for specimen loans. Author would like to thank our reviewers for their insightful comments. This research was funded by Sigma Xi Grants in Aid of Research, Oklahoma State University Robberson Summer Graduate Research Fellowship, Oklahoma State University Women's Faculty Council Research Award, and Oklahoma State University Center for Health Sciences.

## AUTHOR CONTRIBUTIONS

**Leigha Lynch:** Conceptualization; data curation; formal analysis; funding acquisition; methodology; writing-original draft; writing-review and editing. **Haley O'Brien:** Conceptualization; methodology; writing-review and editing. **Ryan Felice:** Methodology; writing-review and editing.

## ORCID

*Leigha M. Lynch* https://orcid.org/0000-0003-3055-8438
*Haley D. O'Brien* https://orcid.org/0000-0002-8758-6571

## REFERENCES

Abaad, M., Tuset, V. M., Montero, D., Lombarte, A., Otero-Ferrer, J. L., & Haroun, R. (2016). Phenotypic plasticity in wild marine fishes associated with fish-cage aquaculture. *Hydrobiologia*, *765*, 343–358.

Adams, D. C. (2014a). A generalized K statistic for estimating phylogenetic signal from shape and other high-dimensional multivariate data. *Systematic Biology*, *63*, 685–697.

Adams, D. C. (2014b). Quantifying and comparing phylogenetic evolutionary rates for shape and other high-dimensional phenotypic data. *Systematic Biology*, *63*, 166–177.

Adams, D. C., & Collyer, M. L. (2018). Multivariate phylogenetic comparative methods: Evaluations, comparisons, and recommendations. *Systematic Biology*, *67*, 14–31.

Adams DC, Collyer ML, Kaliontzopoulou A, Sherratt E. 2017. Geomorph: software for geometric morphometric analyses. In: R package version 3.0.5.

Adams, D. C., & Nistri, A. (2010). Ontogenetic convergence and evolution of foot morphology in European cave salamanders (family: Plethodontidae). *BMC Evolutionary Biology*, *10*, 216.

Adams, K. D., & Rhodes, E. J. (2019). Late Holocene paleohydrology of Walker Lake and the Carson sink in the western Great Basin, Nevada, USA. *Quaternary Research*, *92*, 165–182.

Aguilar-Medrano, R., & Calderon-Aguilera, L. E. (2016). Redundancy and diversity of functional reef fish groups of the Mexican eastern Pacific. *Marine Ecology*, *37*, 119–133.

Allison, I. S. (1982). Geology of pluvial Lake Chewaucan, Lake County, Oregon. *Studies in Geology*, *11*, 1–79.

Álvarez, A., Ercoli, M. D., & Prevosti, F. J. (2013). Locomotion in some small to medium-sized mammals: A geometric morphometric analysis of the penultimate lumbar vertebra, pelvis and hindlimbs. *Zoology*, *116*, 356–371.

Alves, V. M., Moura, M. O., & de Carvalho, C. J. B. (2016). Wing shape is influenced by environmental variability in *Polietina orbitalis* (stein) (Diptera: Muscidae). *Revista Brasileira de Entomologia*, *60*, 150–156.

Andrews, C. A. (2010). Natural selection, genetic drift, and gene flow do not act in isolation in natural populations. *Nature Education Knowledge*, *3*, 1–5.

Andruskiw, M., Fryxell, J. M., Thompson, I. D., & Baker, J. A. (2008). Habitat-mediated variation in predation risk by the American marten. *Ecology*, *89*, 2273–2280.

Arbogast, B. S., Browne, R. A., & Weigl, P. D. (2001). Evolutionary genetics and pleistocene biogeography of north American tree squirrels (*Tamiasciurus*). *Journal of Mammalogy*, *82*, 302–319.

Bacon, S. N., Lancaster, N., Stine, S., Rhodes, E. J., & McCarley Holder, G. A. (2018). A continuous 4000-year lake-level record of Owens Lake, south-Central Sierra Nevada, California, USA. *Quaternary Research*, *90*, 276–302.

Banfield, A. W. F. (1974). *Mammals of Canada*. Toronto, Canada: University of Toronto Press.

Behrensmeyer, A. K., & Turner, A. (2013). Taxonomic occurences of *Martes americana* recorded in the Paleobiology database. In *Fossilworks*. http://www.fossilworks.org/.

Bell, C., Lundelius, E. L., Jr., Barnosky, A., Graham, R. W., Lindsay, E., Ruez, D. R., Jr., ... Zakrzewski, R. J. (2004). The Blancan, Irvingtonian, and Rancholabrean mammal ages. In M. O. Woodburne (Ed.), *Late cretaceous and Cenozoic mammals of North America* (pp. 232–315). New York: Columbia University Press.

Ben-David, M., Flynn, R. W., & Schell, D. M. (1997). Annual and seasonal changes in diets of martens: Evidence from stable isotope analysis. *Oecologia*, *111*, 280–291.

Bennett, K. D. (1991). Milankovitch cycles and their effects on species in ecological and evolutionary time. *Paleobiology*, *16*, 11–21.

Blomberg, S. P., Garland, T., Jr., Ives, A. R., & Crespi, B. (2003). Testing for phylogenetic signal in comparative data: Behavioral traits are more labile. *Evolution*, *57*, 717–745.

Bol'shakov, V. N., Vasil'ev, A. G., Vasil'eva, I. A., Gorodilova, Y. V., & Chibiryak, M. V. (2015). Coupled biotopic variation in populations of sympatric rodent species in the southern Urals. *Russian Journal of Ecology*, *46*, 339–344.

Bond, G., Broecker, W., Johnsen, S., McManus, J., Labeyrie, L., Jouzel, J., & Bonani, G. (1993). Correlations between climate records from North Atlantic sediments and Greenland ice. *Nature*, *365*, 143–147.

Botton-Divet, L., Houssaye, A., Herrel, A., Fabre, A.-C., & Cornette, R. (2018). Swimmers, diggers, climbers and more, a study of integration across the mustelids' locomotor apparatus (Carnivora: Mustelidae). *Evolutionary Biology*, *45*, 182–195.

Burnham, K. P., & Anderson, D. R. (2002). *Model selection and multimodel inference: A practical information-theoretic approach*. New York: Springer Science & Business Media.

Burnham, K. P., & Anderson, D. R. (2004). Multimodel inference: Understanding AIC and BIC in model selection. *Sociological Methods & Research*, *33*, 261–304.

Buskirk, S. W. (1983). *The ecology of marten in southcentral Alaska* (p. 131). Alaska: University of Alaska Fairbanks.

Butler, M. A., & King, A. A. (2004). Phylogenetic comparative analysis: A modeling approach for adaptive evolution. *The American Naturalist*, *164*, 683–695.

Ciais, P., Petit, J., Jouzel, J., Lorius, C., Barkov, N., Lipenkov, V., & Nicolaiev, V. (1992). Evidence for an early Holocene climatic

optimum in the Antarctic deep ice-core record. *Climate Dynamics*, *6*, 169–177.

Ciampaglio, C. N., Kemp, M., & McShea, D. W. (2001). Detecting changes in morphospace occupation patterns in the fossil record: Characterization and analysis of measures of disparity. *Paleobiology*, *27*, 695–715.

Clark, P. U., Dyke, A. S., Shakun, J. D., Carlson, A. E., Clark, J., Wohlfarth, B., … McCabe, A. M. (2009). The last glacial maximum. *Science*, *325*, 710–714.

Clark, T. W., Anderson, E., Douglas, C., & Strickland, M. (1987). Martes americana. *Mammalian Species*, *289*, 1–8.

Colella, J. P., Johnson, E. J., & Cook, J. A. (2018). Reconciling molecules and morphology in north American *Martes*. *Journal of Mammalogy*, *99*, 1323–1335.

Colella, J. P., Wilson, R. E., Talbot, S. L., & Cook, J. A. (2018). Implications of introgression for wildlife translocations: The case of north American martens. *Conservation Genetics*, *20*, 153–166.

Cronin, T. M. (2010). Millenial climate events during deglaciation. In *Paleoclimates: Understanding climate change past and present*. New York: Columbia University Press.

Dawson, N. G., Colella, J. P., Small, M. P., Stone, K. D., Talbot, S. L., & Cook, J. A. (2017). Historical biogeography sets the foundation for contemporary conservation of martens (genus *Martes*) in northwestern North America. *Journal of Mammalogy*, *98*, 715–730.

Dawson, N. G., & Cook, J. A. (2012). Behind the genes. In K. B. Aubry, W. J. Zielinski, M. G. Raphael, G. Proulx, & S. W. Buskirk (Eds.), *Biology and conservation of martens, sables, and fishers: A new synthesis* (pp. 23–38). Ithaca: Cornell University Press.

Day, E. H., Hua, X., & Bromham, L. (2016). Is specialization an evolutionary dead end? Testing for differences in speciation, extinction and trait transition rates across diverse phylogenies of specialists and generalists. *Journal of Evolutionary Biology*, *29*, 1257–1267.

Denton, J. S., & Adams, D. C. (2015). A new phylogenetic test for comparing multiple high-dimensional evolutionary rates suggests interplay of evolutionary rates and modularity in lanternfishes (Myctophiformes; Myctophidae). *Evolution*, *69*, 2425–2440.

Dowle, E. J., Morgan-Richards, M., Brescia, F., & Trewick, S. A. (2015). Correlation between shell phenotype and local environment suggests a role for natural selection in the evolution of Placostylus snails. *Molecular Ecology*, *24*, 4205–4221.

Dyke, A. S. (2004). An outline of north American deglaciation with emphasis on central and northern Canada. In J. Ehlers & P. L. Gibbard (Eds.), *Developments in quaternary sciences* (pp. 373–424). Amsterdam: Elsevier.

Dynesius, M., & Jansson, R. (2000). Evolutionary consequences of changes in species' geographical distributions driven by Milankovitch climate oscillations. *Proceedings of the National Academy of Sciences*, *97*, 9115–9120.

Edwards, R. L., Cheng, H., Murrell, M. T., & Goldstein, S. J. (1997). Protactinium-231 dating of carbonates by thermal ionization mass spectrometry: Implications for quaternary climate change. *Science*, *276*, 782–786.

Eldredge, N., & Gould, S. J. (1972). Punctuated equilibria: An alternative to phyletic gradualism. In T. J. M. Schopf (Ed.), *Models in Paleobiology* (pp. 82–115). San Franscisco: Freeman, Cooper, and Co.

Eshelman, R., & Grady, F. (1986). Quaternary vertebrate localities of Virginia and their avian and mammalian fauna. In J. N. McDonald & S. O. Bird (Eds.), *The quaternary of Virginia: A symposium volume: Department of Mines* (pp. 43–71). Charlottesville: Minerals and Energy, Division of Mineral Resources.

Fabre, A., Cornette, R., Slater, G., Argot, C., Peigné, S., Goswami, A., & Pouydebat, E. (2013). Getting a grip on the evolution of grasping in musteloid carnivorans: A three-dimensional analysis of forelimb shape. *Journal of Evolutionary Biology*, *26*, 1521–1535.

Fabre, A. C., Cornette, R., Goswami, A., & Peigné, S. (2015). Do constraints associated with the locomotor habitat drive the evolution of forelimb shape? A case study in musteloid carnivorans. *Journal of Anatomy*, *226*, 596–610.

Fabre, A. C., Cornette, R., Peigné, S., & Goswami, A. (2013). Influence of body mass on the shape of forelimb in musteloid carnivorans. *Biological Journal of the Linnean Society*, *110*, 91–103.

Felsenstein, J. (1973). Maximum-likelihood estimation of evolutionary trees from continuous characters. *American Journal of Human Genetics*, *25*, 471–492.

Feranec, R. S. (2009). Implications of radiocarbon dates from Potter Creek cave, Shasta County, California, USA. *Radiocarbon*, *51*, 931–936.

Flegr, J. (2013). Microevolutionary, macroevolutionary, ecological and taxonomical implications of punctuational theories of adaptive evolution. *Biology Direct*, *8*, 1.

Folland, C. K., Karl, T., & Vinnikov, K. Y. (1990). Observed climate variations and change. In *Climate change: The IPCC scientific assessment* (pp. 201–238). Cambridge: Cambridge University Press.

Foote, M. (1997). The evolution of morphological diversity. *Annual Review of Ecology and Systematics*, *28*, 129–152.

Friedman, S. T., Martinez, C. M., Price, S. A., & Wainwright, P. C. (2019). The influence of size on body shape diversification across indo-Pacific shore fishes. *Evolution*, *73*, 1873–1884.

Fuller, A. K., & Harrison, D. J. (2005). Influence of partial timber harvesting on American martens in north-Central Maine. *Journal of Wildlife Management*, *69*, 710–722.

Funk, D. J., Nosil, P., & Etges, W. J. (2006). Ecological divergence exhibits consistently positive associations with reproductive isolation across disparate taxa. *Proceedings of the National Academy of Sciences of the United States of America*, *103*, 3209–3213.

Futuyma, D. J. (2010). Evolitionary constraint and ecological consequences. *Evolution*, *64*, 1865–1884.

Gill, J. L., Williams, J. W., Jackson, S. T., Lininger, K. B., & Robinson, G. S. (2009). Pleistocene megafaunal collapse, novel plant communities, and enhanced rire regimes in North America. *Science*, *326*, 1100–1103.

Glennon, K. L., & Cron, G. V. (2015). Climate and leaf shape relationships in four *Helichrysum* species from the Eastern Mountain region of South Africa. *Evolutionary Ecology*, *29*, 657–678.

Goswami, A., Binder, W. J., Meachen, J., & O'Keefe, F. R. (2015). The fossil record of phenotypic integration and modularity: A deep-time perspective on developmental and evolutionary dynamics. *Proceedings of the National Academy of Sciences*, *112*, 4891–4896.

Gould, S. J. (2002). *The structure of evolutionary theory*. Cambridge: Harvard University Press.

Gould, S. J., Lewontin, R. C., Smith, J. M., & Holliday, R. (1979). The spandrels of san Marco and the Panglossian paradigm: A critique of the adaptationist programme. *Proceedings of the Royal Society B: Biological Sciences*, *205*, 581–598.

Grady, F. (1984). A Pleistocene occurrence of *Geomys* (Rodentia: Geomyidae) in West Virginia. In H. Genoways & M. Dawson (Eds.), *Contributions in quaternary vertebrate paleontology: A volume in memorial to John E. Guilday Carnegie Museum of Natural History Special Publications* (pp. 161–168). Pittsburgh: Carnegie Museum of Natural History Special Publications.

Grohé, C., Tseng, Z. J., Lebrun, R., Boistel, R., & Flynn, J. J. (2016). Bony labyrinth shape variation in extant Carnivora: A case study of Musteloidea. *Journal of Anatomy*, *228*, 366–383.

Guilday, J. E., & Hamilton, H. W. (1978). Ecological significance of displaced boreal mammals in West Virginia caves. *Journal of Mammalogy*, *59*, 176–181.

Hairston, N. G., Ellner, S. P., Geber, M. A., Yoshida, T., & Fox, J. A. (2005). Rapid evolution and the convergence of ecological and evolutionary time. *Ecology Letters*, *8*, 1114–1127.

Hannisdal, B. (2006). Phenotypic evolution in the fossil record: Numerical experiments. *Journal of Geology*, *114*, 133–153.

Hansen, T. F., & Houle, D. (2004). Evolvability, stabilizing selection, and the problem of stasis. In M. Pigliucci & K. Preston (Eds.), *Phenotypic integration* (pp. 130–150). Oxford: Oxford University Press.

Harmon, L. J., Losos, J. B., Jonathan Davies, T., Gillespie, R. G., Gittleman, J. L., Bryan Jennings, W., … Mooers, A. Ø. (2010). Early bursts of body size and shape evolution are rare in comparative data. *Evolution*, *64*, 2385–2396.

Harmon, L. J., Weir, J. T., Brock, C. D., Glor, R. E., & Challenger, W. (2008). GEIGER: Investigating evolutionary radiations. *Bioinformatics*, *24*, 129–131.

Harris, M. A., & Steudel, K. (1997). Ecological correlates of hindlimb length in the Carnivora. *Journal of Zoology*, *241*, 381–408.

Hassanin, A. (2015). The role of Pleistocene glaciations in shaping the evolution of polar and brown bears. Evidence from a critical review of mitochondrial and nuclear genome analyses. *Comptes Rendus Biologies*, *338*, 494–501.

Hendry, A. P., Farrugia, T. J., & Kinnison, M. T. (2008). Human influences on rates of phenotypic change in wild animal populations. *Molecular Ecology*, *17*, 20–29.

Hewitt, G. M. (1996). Some genetic consequences of ice ages, and their role in divergence and speciation. *Biological Journal of the Linnean Society*, *58*, 247–276.

Hewitt, G. M. (2004). Genetic consequences of climatic oscillations in the quaternary. *Philosophical Transactions of the Royal Society B: Biological Sciences*, *359*, 183–195.

Hoberg, E., Koehler, A., & Cook, J. (2012). Complex host–parasite systems in *Martes*: Implications for conservation biology of endemic faunas. In K. B. Aubry, W. J. Zielinski, M. G. Raphael, G. Proulx, & S. W. Buskirk (Eds.), *Biology and conservation of martens, sables and fishers: A new synthesis* (pp. 39–57). Ithaca: Cornell University Press.

Holmes, E. B. (1977). Is specialization a dead end? *The American Naturalist*, *111*, 1021–1026.

Huang, J.-P. (2020). Is population subdivision different from speciation? From phylogeography to species delimitation. *Ecology and Evolution*, *10*, 6890–6896.

Hughes, S. S. (2009). Noble marten (*Martes americana nobilis*) revisited: Its adaptation and extinction. *Journal of Mammalogy*, *90*, 74–92.

Hunt, G. (2006). Fitting and comparing models of phyletic evolution: Random walks and beyond. *Paleobiology*, *32*, 578–601, 524.

Hunt, G., Hopkins, M. J., & Lidgard, S. (2015). Simple versus complex models of trait evolution and stasis as a response to environmental change. *Proceedings of the National Academy of Sciences*, *112*, 4885–4890.

Hunt, G., & Rabosky, D. L. (2014). Phenotypic evolution in fossil species: Pattern and process. *Annual Review of Earth and Planetary Sciences*, *42*, 421–441.

Huxley, J. S. (1932). *Problems of relative growth*. New York: L. MacVeagh.

Ives, A. R., Midford, P. E., & Garland, T., Jr. (2007). Within-species variation and measurement error in phylogenetic comparative methods. *Systematic Biology*, *56*, 252–270.

Jackson, S. T., & Overpeck, J. T. (2000). Responses of plant populations and communities to environmental changes of the late quaternary. *Paleobiology*, *26*, 194–220.

Jackson, S. T., Webb, R. S., Anderson, K. H., Overpeck, J. T., Webb Iii, T., Williams, J. W., & Hansen, B. C. S. (2000). Vegetation and environment in eastern North America during the last glacial maximum. *Quaternary Science Reviews*, *19*, 489–508.

Kilbourne, B. M. (2017). Selective regimes and functional anatomy in the mustelid forelimb: Diversification toward specializations for climbing, digging, and swimming. *Ecology and Evolution*, *7*, 8852–8863.

Kinnison, M. T., & Hairston, N. G. (2007). Eco-evolutionary conservation biology: Contemporary evolution and the dynamics of persistence. *Functional Ecology*, *21*, 444–454.

Kinnison, M. T., & Hendry, A. P. (2001). The pace of modern life II: From rates of contemporary microevolution to pattern and process. In A. P. Hendry & M. T. Kinnison (Eds.), *Microevolution rate, pattern, process* (pp. 145–164). Dordrecht: Springer Netherlands.

Klingenberg, C. P. (1998). Heterochrony and allometry: The analysis of evolutionary change in ontogeny. *Biological Reviews*, *73*, 79–123.

Koch, P. L., Diffenbaugh, N. S., & Hoppe, K. A. (2004). The effects of late quaternary climate and pCO 2 change on C 4 plant abundance in the south-Central United States. *Palaeogeography Palaeoclimatology Palaeoecology*, *207*, 331–357.

Lang, C., Leuenberger, M., Schwander, J., & Johnsen, S. (1999). 16°C rapid temperature variation in Central Greenland 70,000 years ago. *Science*, *286*, 934–937.

Law, C. J. (2019). Evolutionary shifts in extant mustelid (Mustelidae: Carnivora) cranial shape, body size and body shape coincide with the mid-Miocene climate transition. *Biology Letters*, *15*, 20190155.

Law, C. J., Slater, G. J., & Mehta, R. S. (2018a). Lineage diversity and size disparity in Musteloidea: Testing patterns of adaptive radiation using molecular and fossil-based methods. *Systematic Biology*, *67*, 127–144.

Law, C. J., Slater, G. J., & Mehta, R. S. (2018b). Small and slender: Evolutionary shifts towards elongate body plans within Mustelidae. *Integrative and Comparative Biology*, *58*, 128–128.

Leach, D. (1977). The descriptive and comparative postcranial osteology of marten (*Martes americana* Turton) and fisher (*Martes pennanti* Erxleben): The appendicular skeleton. *Canadian Journal of Zoology*, *55*, 199–214.

Li, J., Huang, J.-P., Sukumaran, J., & Knowles, L. L. (2018). Microevolutionary processes impact macroevolutionary patterns. *BMC Evolutionary Biology*, *18*, 123.

Lisiecki, L. E., & Raymo, M. E. (2005). A Pliocene-Pleistocene stack of 57 globally distributed benthic δ18O records. *Paleoceanography*, *20*, 1–17.

Lister, A. M. (2004). The impact of quaternary ice ages on mammalian evolution. *Philosophical Transactions of the Royal Society B: Biological Sciences*, *359*, 221–241.

Loehr, J., Worley, K., Grapputo, A., Carey, J., Veitch, A., & Coltman, D. W. (2006). Evidence for cryptic glacial refugia from north American mountain sheep mitochondrial DNA. *Journal of Evolutionary Biology*, *19*, 419–430.

Long, C. A. (1971). Significance of the late Pleistocene fauna from the little box elder cave, Wyoming, to studies of zoogeography of recent mammals. *Great Basin Naturalist*, *31*, 93–105.

Lovette, I. J. (2005). Glacial cycles and the tempo of avian speciation. *Trends in Ecology & Evolution*, *20*, 57–59.

Lyman, R. L. (2011). Paleoecological and biogeographical implications of late Pleistocene noble marten (*Martes americana nobilis*) in eastern Washington state, USA. *Quaternary Research*, *75*, 176–182.

Lynch, L. M. (2019a). Fossil calibration of mitochondrial phylogenetic relationships of north American pine martens, *Martes*, suggests an older divergence of M. americana and *M. caurina* than previously hypothesized. *Journal of Mammalian Evolution*. *27*, 535–548.

Lynch, L. M. (2019b). Limb skeletal morphology of north American pine martens, *Martes americana* and *Martes caurina*, correlates with biome and climate. *Biological Journal of the Linnean Society*, *126*, 240–255.

Mayr, E. (1942). *Systematics and the origin of species*. New York: Columbia University Press.

Meachen, J. A., Dunn, R. H., & Werdelin, L. (2015). Carnivoran postcranial adaptations and their relationships to climate. *Ecography*, *38*, 1–8.

Meachen-Samuels, J. A. (2012). Morphological convergence of the prey-killing arsenal of sabertooth predators. *Paleobiology*, *38* (1), 14.

Meachen-Samuels, J. A., & Van Valkenburgh, B. (2009). Forelimb indicators of prey-size preference in the Felidae. *Journal of Morphology*, *270*, 729–744.

Mead, J. I., Heaton, T. H., & Mead, E. M. (1989). Late quaternary reptiles from two caves in the east-central Great Basin. *Journal of Herpetology*, *23*, 186–189.

Merriam, C. H. (1890). Description of a new marten (*Mustela caurina*) from the northwest coast region of the United States. In *North American Fauna* (pp. 27–30). Washington: US Government Printing Office.

Meyers, J. I. (2007). *Basicranial analysis of Martes and the extinct Martes nobilis (Carnivora: Mustelidae) using geometric morphometrics*. In. Flagstaff: Northern Arizona University.

Milá, B., Smith, T. B., & Wayne, R. K. (2007). Speciation and rapid phenotypic differentiation in the yellow-rumped warbler *Dendroica coronata* complex. *Molecular Ecology*, *16*, 159–173.

Mitteroecker, P., Gunz, P., Bernhard, M., Schaefer, K., & Bookstein, F. L. (2004). Comparison of cranial ontogenetic trajectories among great apes and humans. *Journal of Human Evolution*, *46*, 679–698.

Moriarty, K. M., Epps, C. W., Betts, M. G., Hance, D. J., Bailey, J., & Zielinski, W. J. (2015). Experimental evidence that simplified forest structure interacts with snow cover to influence functional connectivity for Pacific martens. *Landscape Ecology*, *30*, 1865–1877.

Morlo, M., & Peigné, S. (2010). Molecular and morphological evidence for Ailuridae and a review of its genera. In A. Goswami & A. R. Friscia (Eds.), *Carnivoran evolution: New views on phylogeny, form, and function* (pp. 92–140). New York: Cambridge University Press.

Münkemüller, T., Lavergne, S., Bzeznik, B., Dray, S., Jombart, T., Schiffers, K., & Thuiller, W. (2012). How to measure and test phylogenetic signal. *Methods in Ecology and Evolution*, *3*, 743–756.

Muñoz-Fuentes, V., Darimont, C. T., Wayne, R. K., Paquet, P. C., & Leonard, J. A. (2009). Ecological factors drive differentiation in wolves from British Columbia. *Journal of Biogeography*, *36*, 1516–1531.

Near, T. J., Dornburg, A., Kuhn, K. L., Eastman, J. T., Pennington, J. N., Patarnello, T., ... Jones, C. D. (2012). Ancient climate change, antifreeze, and the evolutionary diversification of Antarctic fishes. *Proceedings of the National Academy of Sciences*, *109*, 3434–3439.

Noble, P. J., Ball, G. I., Zimmerman, S. H., Maloney, J., Smith, S. B., Kent, G., ... Driscoll, N. (2016). Holocene paleoclimate history of fallen leaf Lake, CA., from geochemistry and sedimentology of well-dated sediment cores. *Quaternary Science Reviews*, *131*, 193–210.

Nowak, R. M. (1999). *Walker's mammals of the world* (6th ed.). Baltimore: Johns Hopkins University Press.

Oakley, T. H., Gu, Z., Abouheif, E., Patel, N. H., & Li, W.-H. (2004). Comparative methods for the analysis of gene-expression evolution: An example using yeast functional genomic data. *Molecular Biology and Evolution*, *22*, 40–50.

Olson, D. M., Dinerstein, E., Wikramanayake, E. D., Burgess, N. D., Powell, G. V. N., Underwood, E. C., ... Kassem, K. R. (2001). Terrestrial ecoregions of the world: A new map of life on earth: A new global map of terrestrial ecoregions provides an innovative tool for conserving biodiversity. *Bioscience*, *51*, 933–938.

Pagel, M. (1999). Inferring the historical patterns of biological evolution. *Nature*, *401*, 877–884.

Pagel, M., & Meade, A. (2006). Bayesian analysis of correlated evolution of discrete characters by reversible-jump markov chain Monte Carlo. *The American Naturalist*, *167*, 808–825.

Panciroli, E., Janis, C., Stockdale, M., & Martín-Serra, A. (2017). Correlates between calcaneal morphology and locomotion in extant and extinct carnivorous mammals. *Journal of Morphology*, *278*, 1333–1353.

Paradis, E. (2015). An introduction to the phylogenetic comparative methods. In L. Z. Garamszegi (Ed.), *Modern phylogenetic comparative methods and their application in evolutionary biology* (pp. 3–18). Verlag Berlin Heidelberg: Springer.

Paradis, E., Claude, J., & Strimmer, K. (2004). APE: Analyses of Phylogenetics and evolution in R language. *Bioinformatics*, *20*, 289–290.

Polly, P. D. (2008). Adaptive zones and the pinniped ankle: A three-dimensional quantitative analysis of carnivoran tarsal evolution. In E. J. Sargis & M. Dagosto (Eds.), *Mammalian evolutionary morphology* (pp. 167–196). Dordrecht: Springer.

Polly, P. D. (2010). Tiptoeing through the trophics: Geographic variation in carnivoran locomotor ecomorphology in relation to environment. In A. Goswami & A. Friscia (Eds.), *Carnivoran evolution: New views on phylogeny, form, and function* (pp. 374–401). Cambridge: Cambridge University Press.

R Core Team. (2015). *R: A language and environment for statistical computing*. Vienna, Austria: R Foundation for Statistical Computing.

Rahmstorf, S. (2002). Ocean circulation and climate during the past 120,000 years. *Nature*, *419*, 207–214.

Rensch, B. (1959). *Evolution above the species level*. New York: Columbia University Press.

Revell, L. J. (2012). Phytools: An R package for phylogenetic comparative biology (and other things). *Methods in Ecology and Evolution*, *3*, 217–223.

Revell, L. J., Harmon, L. J., & Collar, D. C. (2008). Phylogenetic signal, evolutionary process, and rate. *Systematic Biology*, *57*, 591–601.

Reznick, D., & Travis, J. (2001). Adaptation. In C. W. Fox, D. A. Roff, & D. J. Fairbairn (Eds.), *Evolutionary ecology*. Oxford: Oxford University Press.

Rolian, C. (2019). Ecomorphological specialization leads to loss of evolvability in primate limbs. *Evolution* n/a. *74*, 702–715.

Rosindell, J., Harmon, L. J., & Etienne, R. S. (2015). Unifying ecology and macroevolution with individual-based theory. *Ecology Letters*, *18*, 472–482.

Rovey, C. W., & Balco, G. (2011). Summary of early and middle Pleistocene glaciations in northern Missouri, USA. In J. Ehlers, P. L. Gibbard, & P. D. Hughes (Eds.), *Developments in quaternary sciences* (pp. 553–561). Amsterdam: Elsevier.

Rüber, L., & Adams, D. C. (2001). Evolutionary convergence of body shape and trophic morphology in cichlids from Lake Tanganyika. *Journal of Evolutionary Biology*, *14*, 325–332.

Runck, A. M., & Cook, J. A. (2005). Postglacial expansion of the southern red-backed vole (*Clethrionomys gapperi*) in North America. *Molecular Ecology*, *14*, 1445–1456.

Rundle, H. D., & Nosil, P. (2005). Ecological speciation. *Ecology Letters*, *8*, 336–352.

Samuels, J. X., Meachen, J. A., & Sakai, S. A. (2013). Postcranial morphology and the locomotor habits of living and extinct carnivorans. *Journal of Morphology*, *274*, 121–146.

Schluter, D. (2000). *The ecology of adaptive radiation*. Oxford: Oxford University Press.

Seierstad, I. K., Abbott, P. M., Bigler, M., Blunier, T., Bourne, A. J., Brook, E., … Cook, E. (2014). Consistently dated records from the Greenland GRIP, GISP2 and NGRIP ice cores for the past 104 ka reveal regional millennial-scale δ 18 O gradients with possible Heinrich event imprint. *Quaternary Science Reviews*, *106*, 29–46.

Shackleton, N. J., Sánchez-Goñi, M. F., Pailler, D., & Lancelot, Y. (2003). Marine isotope substage 5e and the Eemian interglacial. *Global and Planetary Change*, *36*, 151–155.

Shafer, A. B. A., Côté, S. D., & Coltman, D. W. (2011). Hot spots of genetic diversity descended from multiple Pleistocene refugia in an apline ungulate. *Evolution*, *65*, 125–138.

Shafer, A. B. A., Cullingham, C. I., CÔTÉ, S. D., & Coltman, D. W. (2010). Of glaciers and refugia: A decade of study sheds new light on the phylogeography of northwestern North America. *Molecular Ecology*, *19*, 4589–4621.

Simons, A. M. (2002). The continuity of microevolution and macroevolution. *Journal of Evolutionary Biology*, *15*, 688–701.

Simpson, G. G. (1944). *Tempo and mode in evolution*. New York: Columbia University Press.

Sinclair, W. J. (1907). *The exploration of the Potter Creek cave*. Oakland: University of California Press.

Slater, G. J., Price, S. A., Santini, F., & Alfaro, M. E. (2010). Diversity versus disparity and the radiation of modern cetaceans. *Proceedings of the Royal Society B: Biological Sciences*, *277*, 3097–3104.

Spanbauer, T. L., Fritz, S. C., & Baker, P. A. (2018). Punctuated changes in the morphology of an endemic diatom from Lake Titicaca. *Paleobiology*, *44*, 89–100.

Steventon, J. D., & Major, J. T. (1982). Marten use of habitat in a commercially clear-cut forest. *Journal of Wildlife Management*, *46*, 175–182.

Stirling, C. H., Esat, T. M., Lambeck, K., & McCulloch, M. T. (1998). Timing and duration of the last interglacial: Evidence for a restricted interval of widespread coral reef growth. *Earth and Planetary Science Letters*, *160*, 745–762.

Stone, K. D., & Cook, J. A. (2002). Molecular evolution of Holarctic martens (genus *Martes*, Mammalia: Carnivora: Mustelidae). *Molecular Phylogenetics and Evolution*, *24*, 169–179.

Stone, K. D., Flynn, R. W., & Cook, J. A. (2002). Post-glacial colonization of northwestern North America by the forest-associated American marten (*Martes americana*, Mammalia: Carnivora: Mustelidae). *Molecular Ecology*, *11*, 2049–2063.

Tankersley, K. B. (1997). Sheriden: A Clovis cave site in eastern North America. *Geoarchaeology*, *12*, 713–724.

Thompson RS, Anderson KH, Bartlein PJ. 1999. Quantitative Paleoclimatic Reconstructions from Late Pleistocene Plant Macrofossils of the Yucca Mountain Region: US Department of the Interior, US Geological Survey.

Voje, K. L. (2016). Tempo does not correlate with mode in the fossil record. *Evolution*, *70*, 2678–2689.

Voje, K. L., Hansen, T. F., Egset, C. K., Bolstad, G. H., & Pelabon, C. (2014). Allometric constraints and the evolution of allometry. *Evolution*, *68*, 866–885.

Wake, D. B., Roth, G., & Wake, M. H. (1983). On the problem of stasis in organismal evolution. *Journal of Theoretical Biology*, *101*, 211–224.

Weber, M. G., Mitko, L., Eltz, T., & Ramírez, S. R. (2016). Macroevolution of perfume signalling in orchid bees. *Ecology Letters*, *19*, 1314–1323.

Weir, J. T., & Schluter, D. (2004). Ice sheets promote speciation in boreal birds. *Proceedings of the Royal Society B: Biological Sciences*, *271*, 1881–1887.

Wetmore, A. (1962). Notes on fossil and subfossil birds. *Smithsonian miscellaneous collections.*, *145*, 1–17.

Wilkins, D. E., & Currey, D. R. (1999). Radiocarbon chronology and$\delta$13C analysis of mid-to late-Holocene aeolian environments, Guadalupe Mountains National Park, Texas, USA. *The Holocene*, *9*, 363–371.

Williams, J. W., & Jackson, S. T. (2007). Novel climates, no-analog communities, and ecological surprises. *Frontiers in Ecology and the Environment*, *5*, 475–482.

Williams, J. W., Shuman, B. N., & Webb, T. (2001). Dissimilarity analyses of late-quaternary vegetation and climate in eastern North America. *Ecology*, *82*, 3346–3362.

Wolff, E. W., Chappellaz, J., Blunier, T., Rasmussen, S. O., & Svensson, A. (2010). Millennial-scale variability during the last glacial: The ice core record. *Quaternary Science Reviews*, *29*, 2828–2838.

Young, N. M., & Hallgrímsson, B. (2005). Serial homology and the evolution of mammalian limb covariation structure. *Evolution*, *59*, 2691–2704.

Youngman, P. M., & Schueler, F. W. (1991). *Martes nobilis* is a synonym of *Martes americana*, not an extinct Pleistocene-Holocene species. *Journal of Mammalogy*, *72*, 567–577.

Yuan, F., Koran, M. R., & Valdez, A. (2013). Late glacial and holocene record of climatic change in the southern Rocky Mountains from sediments in San Luis Lake, Colorado, USA. *Palaeogeography Palaeoclimatology Palaeoecology*, *392*, 146–160.

Zelditch, M. L., Swiderski, D. L., & Sheets, H. D. (2012). *Geometric Morphometrics for biologists: A primer*. London: Academic Press.

Zielinski, W. J., & Duncan, N. P. (2004). Diets of sympatric populations of American martens (*Martes americana*) and fishers (*Martes pennanti*) in California. *Journal of Mammalogy*, *85*, 470–477.

Zink, R. M., & Dittmann, D. L. (1993). Gene flow, refugia, and evolution of geographic variation in the song sparrow (*Melospiza melodia*). *Evolution*, *47*, 717–729.

Zrzavý, J., & Řičánková, V. (2004). Phylogeny of recent Canidae (Mammalia, Carnivora): Relative reliability and utility of morphological and molecular datasets. *Zoologica Scripta*, *33*, 311–333.

## SUPPORTING INFORMATION

Additional supporting information may be found online in the Supporting Information section at the end of this article.

**How to cite this article:** Lynch LM, Felice R, O'Brien HD. Appendicular skeletal morphology of North American *Martes* reflect independent modes of evolution in conjunction with Pleistocene glacial cycles. *Anat Rec*. 2020;1–24. https://doi.org/10.1002/ar.24545